

**AUGMENTED REALITY TRAINING PLATFORM FOR
PLACEMENT OF NEUROSURGICAL BURR HOLES**

by

Zachary Michael Cieman Baum

A thesis submitted to the School of Computing
in conformity with the requirements for
the degree of Master of Science

Queen's University

Kingston, Ontario, Canada

April, 2019

Copyright © Zachary Michael Cieman Baum, 2019

Abstract

Augmented reality has been used in neurosurgery to aid in the visualization of lesions, though it has not been widely adopted for simulation-based neurosurgical training. This work aims to determine if augmented reality can improve identification of drill location and drill angle for neurosurgical procedures and to define objective metrics for assessing trainee performance.

An augmented reality visualization system was developed using the *Microsoft HoloLens*. Trainee performance metrics were defined and validated intra-operatively in fifteen neurosurgical cases by attending neurosurgeons and trainees. Trainee performance in localization of drill location and angle tasks was assessed in a simulated training with augmented reality visualization and compared with two other visualization methods.

The proposed metrics allowed us to significantly differentiate levels of competence between attending neurosurgeons and trainees in identification of drill location with ($p = 0.011$) and without ($p = 0.001$) the *HoloLens* and drill angle with ($p = 0.032$) the *HoloLens*. Augmented reality visualization significantly improved trainee performance in localization of drill location ($p < 0.001$ and $p = 0.008$) and angle ($p < 0.001$ and $p < 0.001$) in comparison to two other visualization methods. Trainees rated augmented reality visualization equally or more helpful compared to the two other visualization methods.

Trainee performance assessment with augmented reality visualization and the proposed performance metrics stands to add practical value to neurosurgical training curricula. This work represents a necessary step in curriculum development in neurosurgical training for the task of drill location and angle localization in a variety of neurosurgical procedures.

Co-Authorship

The work presented in this thesis was completed under the supervision of Dr. Gabor Fichtinger.

Additional guidance was received from Dr. Andras Lasso, Dr. Tamas Ungi, and Dr. Ron Levy.

This work also appears in the following publications:

- Zachary Baum, Andras Lasso, Emily Rae, Sarah Ryan, Tamas Ungi, Ron Levy, Gabor Fichtinger. “An augmented reality training platform for neurosurgical burr hole localization,” (Submitted).
- Zachary Baum, Sarah Ryan, Emily Rae, Andras Lasso, Tamas Ungi, Ron Levy, Gabor Fichtinger. “Assessment of intraoperative neurosurgical planning with the Microsoft HoloLens,” *17th Annual Imaging Network of Ontario Symposium*, Toronto, Canada, March 28-29, 2019.

Acknowledgements

I would like to thank and express my appreciation to my supervisor, Dr. Gabor Fichtinger. His knowledge, patience and willingness to take me under his wing as a student in the Laboratory for Percutaneous Surgery (Perk Lab) for the past several years had added immense value to my time at Queen's and to my academic experiences. He almost singlehandedly encouraged me to pursue research, and when all is said and done, I could not have hoped for a better time working in the Perk Lab.

Though not my supervisors, I have been extremely lucky to have had the opportunity to work alongside and with guidance from Dr. Tamas Ungi, Dr. Andras Lasso, and Dr. Ron Levy in this work. Without their guidance, support, and skills, much of the work outlined here, and much of what I have accomplished in the past several years, would not have been possible. They are patient teachers, incredible mentors, and are always willing to explain and demonstrate concepts several times over.

I would like to thank all my other colleagues and students in the Perk Lab, of whom there are too many to name, for their support and encouragement. I am grateful for all those in the Queen's School of Computing, the Faculty of Arts and Science, the School of Graduate Studies and at Queen's University who have supported me, my studies, and my many other endeavours.

Countless friends and family have helped me through not only the past two years with this work – but through the past six years that I've spent at Queen's University. Without their support, I would not have made it through my time at Queen's, achieving as much as I have – all of my success is shared with you.

Table of Contents

Abstract	ii
Co-Authorship	iii
Acknowledgements	iv
List of Figures	vii
List of Tables	ix
List of Abbreviations	x
Chapter 1 Introduction.....	1
1.1 Medical Imaging Modalities.....	1
1.2 Freehand Image-Guided Interventions	2
1.3 Computer-Assisted Navigation Systems	4
1.3.1 Electromagnetically Tracked Navigation Systems	5
1.3.2 Optically Tracked Navigation Systems	5
1.3.3 Software Platforms for Surgical Navigation	7
1.4 Augmented Reality Surgical Navigation Systems.....	9
1.4.1 Video Projection-Based Systems.....	10
1.4.2 CT / MRI-Based Overlay Systems	11
1.4.3 Mobile CT / MRI-Based Image Overlay Systems.....	14
1.4.4 Head-Mounted Video Display Systems	14
1.4.5 Head-Mounted Optical Display Systems	16
1.4.6 Navigation System Development on Commercial Platforms	16
1.5 The Microsoft HoloLens	18
1.5.1 Surgical Guidance and Planning with the Microsoft HoloLens	19
1.6 Clinical Motivation.....	22
1.7 Augmented Reality in Neurosurgery	23
1.8 Competency-Based Medical Education	24
1.8.1 Neurosurgical Residency Programs.....	25
1.9 Objective	26
1.10 Contributions	27
Chapter 2 System Design and Implementation	28
2.1 Software Implementation	28
2.2 Model Creation and Visualization.....	29
2.3 Registration Method	30

2.4 Registration Accuracy and Feasibility Study	32
2.5 Results and Discussion	34
2.6 Summary	37
Chapter 3 Intra-operative Planning and Target Localization	39
3.1 Study Design	39
3.2 Study Participants and Setting	39
3.3 Study Protocol	40
3.4 Experimental Design	41
3.5 Data Processing	44
3.6 Definition and Computation of Performance Metrics	45
3.6.1 Drill-tip Distance	47
3.6.2 Distance to Lesion	48
3.6.3 Drill Angle Error	48
3.6.4 Angle to Lesion	49
3.7 Statistical Analysis	50
3.8 Results and Discussion	50
3.9 Summary	53
Chapter 4 Simulated Target Localization	54
4.1 Study Design	54
4.2 Experimental Setup	54
4.3 Data Processing	56
4.4 Definition and Computation of Performance Metrics	57
4.5 Results and Discussion	58
4.6 Summary	61
Chapter 5 Future Work and Conclusions	63
5.1 Future Work	63
5.2 Conclusions	64
Bibliography	66
Appendix A Copy of Research Ethics Board Approval	74
Appendix B Copy of Research Ethics Board Amendment	77

List of Figures

Figure 1. Various sizes of 6 degree-of-freedom electromagnetic tracking sensors (Left) and electromagnetic transmitter and tracking unit (Right).....	6
Figure 2. Polaris Spectra and Vicra optical tracking systems (Top) and various compatible passive tracking markers (Bottom).	6
Figure 3. Software architectures for open-source computer-assisted navigation systems.	9
Figure 4. Prototype 2D Image Overlay System with overlaid image shown on a simulated patient.	12
Figure 5. 2D Image Overlay System mounted to CT scanner gantry in a percutaneous needle insertion study on a simulated patient.	13
Figure 6. Mobile image overlay system prototype in use for a percutaneous needle insertion study on a phantom thoracic spine.	15
Figure 7. The <i>HoloLens</i> used for insertion of a catheter in an extraventricular drain.	20
Figure 8. The <i>HoloLens</i> as part of the <i>VimedixAR</i> simulated ultrasound medical training system.	20
Figure 9. <i>HoloQuickNav</i> 's Patient Manager showing a preview of all models on the device. This image shows the skin surface, brain, and intra-cortical lesion models. This image was captured with the real-world environment removed from all images to better visualize the user interface.....	29
Figure 10. <i>HoloQuickNav</i> 's main user interface when registering the models to the patient. This image shows the skin surface, brain, and intra-cortical lesion models. This image was captured with the real-world environment removed from all images to better visualize the user interface.....	30
Figure 11. The registration process for <i>HoloQuickNav</i> with (a) the user translating models towards the simulated patient and (b) models in place on the simulated patient relative to the user.....	31
Figure 12. The male plastic phantom (a) without hair and (b) with hair and the female plastic phantom (c) without hair and (d) with hair.....	33
Figure 13. Different ranges of accuracy for self-reported holographic marker placement by users in the registration accuracy and feasibility study.	34
Figure 14. Bar chart assessment of all registration accuracies (left) and box and whisker plot of all registration times (right) for novice and expert participants.	36
Figure 15. Bar chart assessment comparing male and female phantom registration accuracies for novices (left) and experts (right).	36

Figure 16. Neurosurgeon using the *Xbox One Wireless Controller* while wearing the *HoloLens* to register the holographic models to a patient. 42

Figure 17. Trainee (right) using the pointer to indicate the drill location and drill angle while wearing the *HoloLens* as a 3D point cloud of the scene is acquired using the *Intel RealSense D415 Depth Camera* (left). 43

Figure 18. Neurosurgeon (right) using the *HoloLens* to denote the surgical access point and trajectory before commencing surgery. 43

Figure 19. Aligned 3D point clouds in *MeshLab* following a ‘Point Based Glueing’ and ICP registration process. The patient’s face and identifying features, though relevant for the registration process, are blurred in the image. 45

Figure 20. Pointer trajectories, shown in yellow, obtained from aligned 3D point clouds shown on models of the patient’s intra-cortical lesion, brain and skin surface in *3D Slicer*. 46

Figure 21. 3D models of surface anatomy, brain, intra-cortical lesion, and user-defined trajectories from one localization task in the simulated study. The black point shows the lesion’s geometric center; the green line shows the clinical gold-standard drill location and drill angle; the red line shows the participant’s drill location and drill angle; the yellow line shows the trajectory from the participant’s drill location to lesion’s center; the blue line shows the drill-tip distance; the white line shows the distance to lesion; the purple arc shows the drill angle error; the orange arc shows the angle to lesion. 47

Figure 22. Views of visualizations provided to the user in the phantom study while using the (a) 2D Method, (b) 3D Method, and (c) AR Method in an image series used in the study. 55

Figure 23. Views in *3D Slicer* of the phantom head and deformably registered brain and intra-cortical lesion models for one trial of the simulated study showing (a) the target drill location and drill angle (red line) as defined by an attending neurosurgeon, (b) the Markups Fiducials annotating the target within the intra-cortical lesion and the drill location, (c) the participant’s pointer (blue line) denoted drill location and drill angle relative to the target drill location and drill angle, and (d) the Markups Fiducials annotating the pointer-tip and the end of the pointer shaft. 57

Figure 24. Min-max-average assessment of post-study questionnaire responses. 61

List of Tables

Table 1. Registration accuracy results.....	35
Table 2. Registration task completion times.	35
Table 3. 2D and AR method performance comparison.	51
Table 4. Trainee and attending neurosurgeon performance comparison.....	51
Table 5. 2D, 3D, and AR method performance summary.....	58
Table 6. Pairwise performance comparison of 2D, 3D, and AR method target localization metrics.	58

List of Abbreviations

2D Two Dimensions/Dimensional

3D Three Dimensions/Dimensional

AR Augmented Reality

CBME Competency-Based Medical Education

CT Computerized Tomography

DICOM Digital Imaging and Communications in Medicine

HMD Head Mounted Display

ICP Iterative Closest Point

MRI Magnetic Resonance Imaging

OBJ Wavefront .obj File

SLAM Simultaneous Localization and Mapping

STL Stereolithography

XML eXtensible Markup Language

Chapter 1

Introduction

1.1 Medical Imaging Modalities

Computerized Tomography (CT) and Magnetic Resonance Imaging (MRI) have been some of the enabling imaging modalities of image-guided interventions. Image-guided interventions are medical procedures which use computer-based systems to provide virtual images to help the clinician precisely plan, visualize, and target the surgical site [1].

CT imaging uses a series of computer-processed radiographic images, taken in multiple cross-sectional angles, to create three-dimensional (3D) images for diagnostic or therapeutic purposes. These images produce high-quality images of internal structures, bones, tissues and blood vessels. This allows for these images to be used for diagnosing and planning treatments without the need for exploratory surgery. CT imaging is fast, accurate and noninvasive. However, the radiation used during CT scans can damage cells and can predispose to various forms of cancer later in life, especially if patients had frequent CT examinations in childhood [2].

MRI uses magnetic fields and radio waves to generate cross-sectional diagnostic images of internal structures in the body, such as tissues and organs. Compared to CT, MRI imaging provides superior tissue contrast and allows for more accurate discrimination between normal tissue and any pathologic structures. MRI does not emit any ionizing radiation, though the scanning process is typically much longer in duration, and the process is much louder. As such, these scans may render patients uncomfortable as they require patients to enter a narrow and confining tube for extended periods of time.

1.2 Freehand Image-Guided Interventions

A medical intervention involves the use or placement of a surgical instrument for performing aspirations, injections, ablations or targeted therapies – in the case of radiation therapy – to help with the treatment or curing of a medical condition. Performing interventions and procedures under medical image guidance using the previously discussed imaging modalities has become common practice across multiple areas of medicine throughout the developed world. Planning each intervention commences in a different way depending on the imaging modality to be used for guidance. Pre-operative images, such as CT or MRI, can be used to plan surgical interventions to specific target regions in the patient before the procedure starts. Clinicians may often use different types of medical imaging technologies, such as ultrasound or fluoroscopy, intraoperatively to ensure their tools follow a suitable trajectory, and to track their progress towards a target or target regions in the patient. Patient outcomes from non-invasive procedures where planning using pre-operative images occurred versus outcomes from open surgical procedures have shown that pre-planning and using less invasive approaches are more effective for surgeries [3]. Surgical outcomes when using image guidance and surgical pre-planning have also been observed to be better and to improve the overall success of the procedure, as open procedures tend to increase patient discomfort and require longer patient recovery times [4, 5].

However, these freehand procedures often involve images which are displayed off to the side of the patient on a monitor; effectively a basic ergonomic problem which decouples the image from the patient. This means that performing any minimally invasive procedure will require significant hand-eye coordination and concentration on the part of the clinician to mentally overlap the patient and their medical images as a guide for the intervention.

After browsing through preliminary medical images, a target entry point is identified. Using the above mentioned mental overlapping and hand-eye coordination skills, the clinician will place their tool at, what is effectively, their best guess of the target location in the direction of the target

trajectory on the patient. Throughout the intervention, additional images may be acquired to ensure proper trajectories and to visualize progress. Acquisition of multiple confirmation images is known to lead to longer treatment times, increased levels of patient discomfort, and increased patient radiation exposure if CT imaging, or any other type of imaging where ionizing radiation is required, is being used. Work must be done to reduce human-introduced errors in these interventions and surgeries to reduce treatment times, patient discomfort and radiation exposure.

One goal of preoperative planning with medical images has been to aid surgeons in finding an optimal surgical route. The aforementioned medical imaging technologies and computer-based planning methods have allowed clinicians to assess various surgical routes outside the operating room without time pressure. As medical imaging continues to play a crucial role in the growing domain of image-guided interventions and surgeries, advances in imaging technologies are expected to continue expanding the scope of practical clinical applications. Through this expansion, the acceptance of new surgical guidance technologies into clinical settings will continue to be seen by increasingly cost-conscious healthcare providers.

In 2014, the market for image-guided interventions in the United States was valued at over \$753 Million USD, with the market size estimated to surpass 1 Billion USD before the year 2020¹. Interventional and surgical imaging has seen a dramatic rise in growth stemming from the success of these less invasive practices and minimally invasive interventional procedures. The increasing availability of sophisticated informatics-based imaging tools, due in part to the wide domain of applications for which different imaging modalities are now used for, has also greatly contributed.

¹ Grant View Research, *Image-guided Therapy Systems Market Size, Share & Trends Analysis Report By End Use, By Product, By Application, And Segment Forecasts, 2018 – 2025*, accessed 10 March 2019, <https://www.grandviewresearch.com/industry-analysis/image-guided-therapy-systems-market>

1.3 Computer-Assisted Navigation Systems

Computer-assisted navigation systems make use of specialized software to visualize where an operator's surgical tools are relative to the acquired patient images in real-time on a computer screen. These displays have aided in eliminating the need for the cognitively demanding hand-eye coordination which was required of clinicians when performing freehand interventions. Displaying the positions of surgical tools, the patient, and other devices has been able to greatly enhance a clinician's ability to perform freehand image-guided interventions. Such systems have also been able to provide real-time feedback on the position of the instrument relative to the patient's medical images. Owing to the small margins of error that are common in surgery, inexperienced clinicians and residents have favoured planning and navigational aids in the operating room, and as additional learning tools. These tools can help inexperienced clinicians and residents build the foundations of their surgical skills and become increasingly confident with their surgical skills [6]. The perception of safety and level of self-reported confidence experienced by surgeons during procedures also increases as they use these systems because they are able to view their tools in a manipulable and accurate reconstruction of the surgical environment [7, 8].

A basic setup for a computer-assisted surgical navigation system typically uses software and hardware in tandem with either electromagnetically or optically tracked tools to assist in generating the visual enhancements. During the surgery, electromagnetically tracked sensors or optical markers are attached to the patient and any surgical instruments. These systems allow for guidance in procedures by registering a patient's physical location with a previously acquired patient volumetric image [9]. Registration is a process wherein a relationship between the real coordinate system of the patient and the virtual coordinate system of the medical images is established [10]. Registration of patient to their medical images can remove some of the required hand-eye coordination and mental overlapping that is required of clinicians in freehand interventions.

While some aspects of surgical guidance and image-guided navigation are performed without planning or the use of any previously acquired medical images, once the registration process is complete, many neurosurgical and spine procedures will become 'image-based', relying on the patient's imaging to guide the clinician [10]. As discussed previously, areas or objects of interest and the paths to them can be pre-planned before any incisions or tool insertions are made using these images as a map to help the surgeon to effectively navigate through the patient.

1.3.1 Electromagnetically Tracked Navigation Systems

Electromagnetically tracked navigation systems do not require a visual line-of-sight in order to be used, allowing each of the electromagnetic sensors to be placed near the tip of any tracked tools, and closer to the region of interest due to their small size (Figure 1). Electromagnetic sensors use spiral coils in the X, Y and Z directions and the location of the system generated electromagnetic field relative to the coils in real-time to determine their position. However, these sensors are susceptible to field distortion when in the presence of metallic materials and the tools that are used must be wired into the system and tethered to a computer (Figure 1) [11]. These shortcomings have hindered the adoption of electromagnetic tracking systems for clinical use [11].

1.3.2 Optically Tracked Navigation Systems

Optically tracked navigation systems require a line-of-sight to be used in surgical navigation. These systems use stereoscopic cameras or infrared sensors to track active or passive markers which are placed continuously in their field of view to determine their position in real-time and report the position of the tracked surgical tool for the clinician (Figure 2). These markers hold the advantages of being wireless, lightweight, and are not susceptible to field distortion. Furthermore, it has been measured that optically tracked navigation systems are capable of being accurate to under 1 mm and that they are more reliable than electromagnetically tracked navigation systems [12].



Figure 1. Various sizes of 6 degree-of-freedom electromagnetic tracking sensors (Left)² and electromagnetic transmitter and tracking unit (Right)³.



Figure 2. Polaris Spectra and Vicra optical tracking systems (Top) and various compatible passive tracking markers (Bottom).⁴

² Ascension Technology Corporation, *6DOF Sensors*, accessed 1 March 2019, <https://www.ascension-tech.com/products/trakstar-drivebay/>

³ Ascension Technology Corporation, *trakSTAR and Transmitter*, accessed 1 March 2019, <https://www.ascension-tech.com/products/trakstar-drivebay/>

⁴ Northern Digital Incorporated, *Polaris Series*, accessed 1 March 2019, <https://www.ndigital.com/msci/products/polaris-series/>

1.3.3 Software Platforms for Surgical Navigation

The final piece of development in these complex systems is the engineering of existing technologies and imaging modalities into one complete and user-friendly software package. Success in the field has been withheld by unnecessarily expending resources on the reimplementation of what are typically considered common features that already exist or are available in other open-source packages and software [13]. The use of open-source software platforms can allow for the sustained effectiveness of contributions and resources from many research groups to carry on internationally from year-to-year, and project-to-project [13].

In searching for a common platform for computer-assisted surgical navigation, many research groups have jointly focused their efforts on the creation and maintenance of large, open-source projects which allow for academic and commercial use with no restrictions. This collaboration and resource sharing allowed for the development of many tools which are used throughout various systems and technologies that are outlined in the following section. These platforms share the concept that there are developer communities to help in finding (and fixing) problems. They hold a belief that these platforms should be extensible and customizable as needed – without the need for involvement from the original developers [13].

The most popular research application in the medical imaging community is *3D Slicer*⁵ [13]. Built over two decades with the support of many large, international, and collaborative grants and agencies, the *3D Slicer* community has consistently provided a powerful, open-source, and multi-platform tool for researchers and clinicians. Through a web-based extension manager, similar to the ‘App Store’, *3D Slicer* offers multiple different extensions, plugins and sample data which can all be downloaded and installed for free [14]. Several of these extensions, such as *SlicerIGT*⁶, support image-guided navigation for medical interventions through the inclusion of typical tasks

⁵ 3D Slicer, www.slicer.org

⁶ SlicerIGT, www.slicerigt.org

and routines needed for surgical guidance. As *3D Slicer* and *SlicerIGT* do not communicate with hardware devices directly, communication protocols ensure the compatibility between software and hardware.

*OpenIGTLink*⁷ is a simple network communication protocol which is widely accepted and used across most major interventional research applications, and several commercial device manufacturers [13, 15]. For devices that do not natively support the *OpenIGTLink* protocol, there is the *PLUS Toolkit*⁸. The *PLUS toolkit* is capable of transferring information between hardware and system applications – such as *3D Slicer*. By communicating with a wide range of commercial devices that are commonly used in medical interventions, the *PLUS Toolkit* communicates, synchronizes, saves, and transfers data streams to other applications in real-time through the *OpenIGTLink* protocol [16].

Navigation systems are typically divided into three separate layers; hardware abstraction, application platform, and application (Figure 3) [13]. This separation allows for efficient development and deployment of new applications. *OpenIGTLink* and the *PLUS Toolkit* may be used at the hardware abstraction level to gather and synchronize data streams from various medical imaging modalities and tracking systems. *3D Slicer* and *SlicerIGT* may then be used at the application platform level as reusable application components to drive the simplicity in the reimplementation of common features, such as visualization or data processing. Custom applications may then be created to fill the application level. At this level, application specific user interfaces and features can be implemented in only a few hundred lines of code.

⁷ OpenIGTLink, www.openigtlink.org

⁸ PLUS Toolkit, www.plustoolkit.org

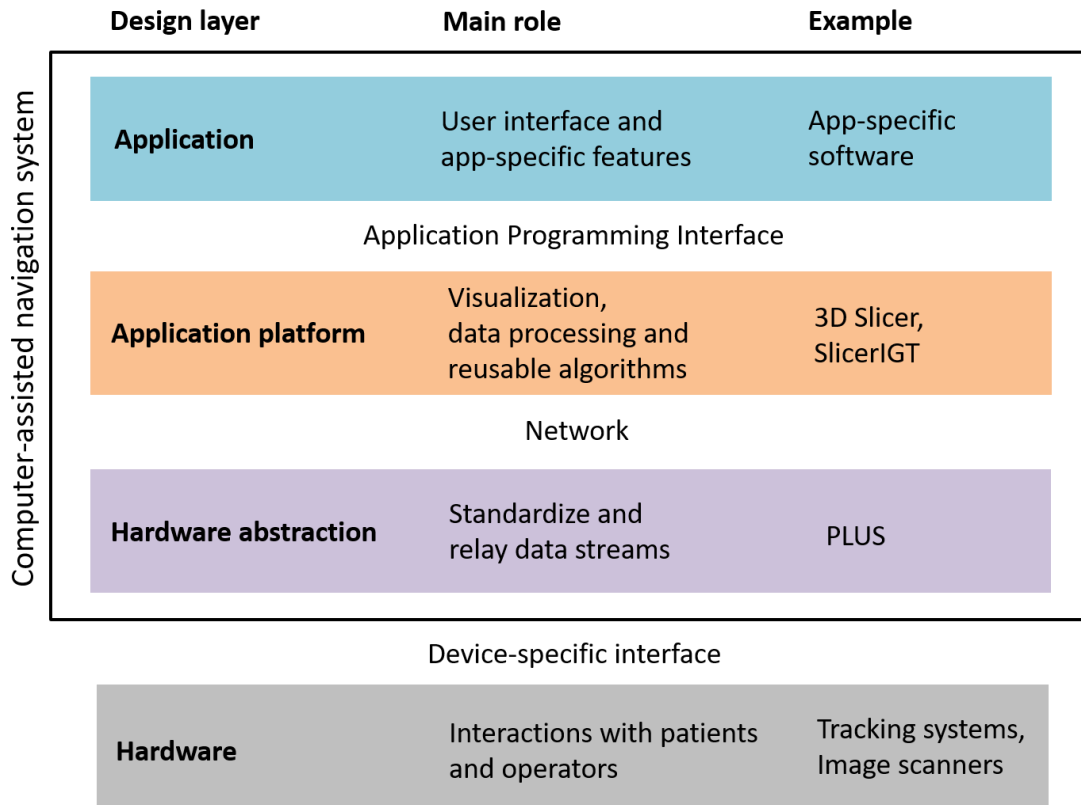


Figure 3. Software architectures for open-source computer-assisted navigation systems.

1.4 Augmented Reality Surgical Navigation Systems

Augmented reality (AR) is a visualization and imaging technology which brings the ability to superimpose data and images into the real world, eliminating the need to mentally reconstruct or project images onto patients. AR systems can enhance the operator’s world with additional information. This is typically accomplished by superimposing computer-generated images, videos or data into the user’s field of view in real-time. AR surgical guidance systems have been proposed as solutions to overcome multiple shortcomings of image-guided surgeries and create a surgeon-patient interface. This is due in part to the fact that these technologies can merge patient images, surgical plans, and the surgeon's field of view into one single visual [17]. AR technologies have been starting to play an increasingly important role in tailoring surgeries to specific patients.

Through the evaluation of surgical strategies and patient outcomes, they have been shown to help reduce the invasiveness of several procedures [17].

One such application of AR in the medical field is producing simulated ‘X-ray vision’, wherein the operator can see through a superimposed CT or MRI volume, and into the operator’s field of view – directly over the patient. In a similar method to the registrations used in tracked navigation systems, images can be registered to the physical location of the patient to ensure the location that images are displayed in the correct scale, location and orientation. From this guiding concept, there are many different tools and applications which have emerged to enhance the clinician’s view by superimposing volumetric images directly on the patient. These methods have typically employed some combination of video or holographic images coupled with head-mounted displays (HMD) or projectors; such as Blackwell *et al.*’s tracked head-mounted volumetric overlay display [18]. These systems typically required extensive calibration, registration, and tracking of all hardware components, as well as any handheld tools, for proper operation and use of each respective system.

1.4.1 Video Projection-Based Systems

Video-based and projection-based displays have been used to display acquired images onto a HMD in front of the operator, or on a frame above the operators’ viewpoint. By using a camera and real-time video during the procedure, pre-operative CT or MRI images were projected on these displays. There have been two commonly implemented types of projection-based displays:

- Those which display video directly to the operator through a headset or other HMD;
- Those which display projected images directly onto the patient space.

Video-based displays made use of live video streams from multiple head-mounted stereo cameras to display a real-time video on the screen in front of the operator. The operator was then able to move freely around in space [19] and have these displays to provide additional patient or medical data, in addition to the live video [20]. In the realm of projection-based image displays, through

systems such as the *Varioscope AR* [21], clinicians could see a reflected patient image and the physical object on and through the semi-transparent mirrors, as provided by the HMD [21]. These systems required constant tracking of the clinician's head, and any handheld tools during the procedure. These systems all required complex registration procedures to ensure that the head mounts, handheld tools, camera, and patient images were properly aligned during use. Additionally, as the user was required to focus not only on the display near the eyes but on the patient as well, these types of systems were known to cause discomfort when in use for prolonged periods. Both limitations rendered the effective clinical translation of such systems difficult.

Projection based systems were proposed to remove the need for any additional displays to be in the surgeon's field of view. These systems came with the added benefit of no longer requiring head, gaze or positional tracking. By projecting preoperative models and images directly on the patient, the computer screen's images and patient become fused as in the *Augmented Reality Computer Assisted Spine Surgery (ARCASS)* system [22]. Using the projection, 3D patient models could be overlaid onto the patient with any relevant anatomy, entry points, target points, and other surgical annotations clearly indicated and visible. The ARCASS was able to reduce procedure duration by 70% compared to conventional methods – and as a result of not requiring the use of intra-operative imaging, possible intra-operative radiation exposure was negligible [22]. However, there were limitations associated with the projection system. Images could only be displayed in one plane. Furthermore, because the image was projected from above, any intrusion from the clinicians would occlude the projected image and prevent the clinician from being able to view the image while directly over the patient.

1.4.2 CT / MRI-Based Overlay Systems

In trying to design a simpler AR system for medical applications, various two-dimensional (2D) image overlay systems were developed. These systems used a single volumetric image and overlaid it directly onto the patient using a 'mirror-monitor' configuration. This image overlay consisted of

a display monitor and a semi-transparent mirror that were fixed together to reflect the screen image down to be superimposed on the patient in the correct location in space. As such, image overlay systems allowed operators to see their target and then insert their needle in a similar way to how they would be able to insert a needle into a transparent material (Figure 4) [23].

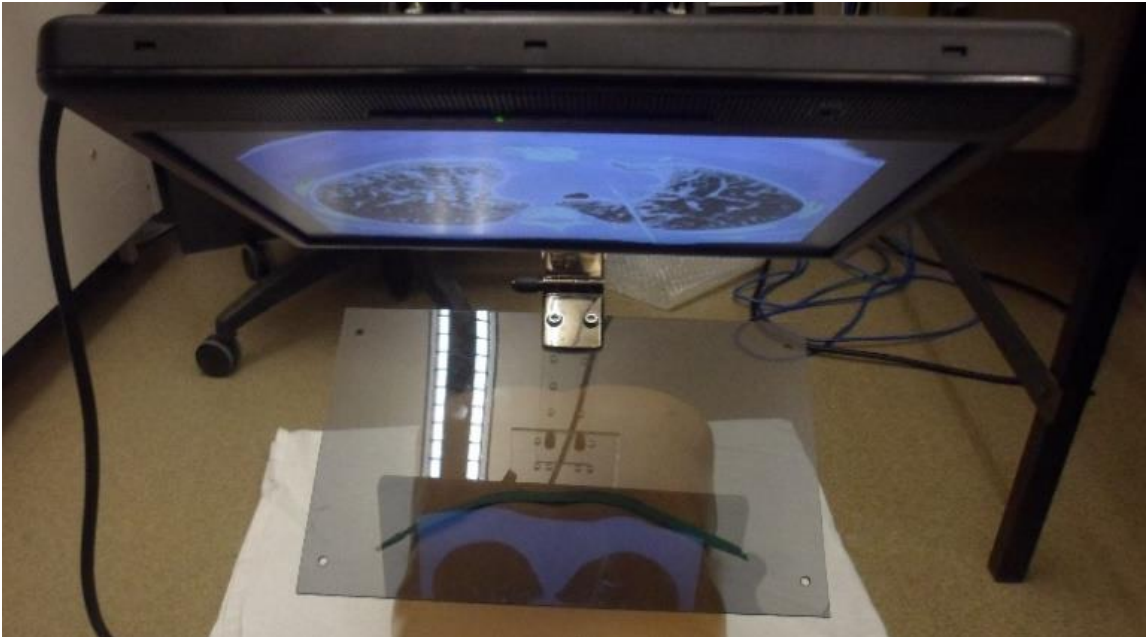


Figure 4. Prototype 2D Image Overlay System with overlaid image shown on a simulated patient.⁹ Such systems required no head tracking or projection of images and came with the added benefit that they allowed multiple operators to view the overlaid image through the system's semi-transparent mirror at the same time. However, the image overlay system had to be mounted and aligned to the CT scanner to generate an AR image for guiding interventions (Figure 5) [23, 24] and required a tedious and sensitive calibration process to properly align the overlaid image plane.

⁹ Unpublished image; see [23] and [24] for further details and additional images about this, and similar, systems.

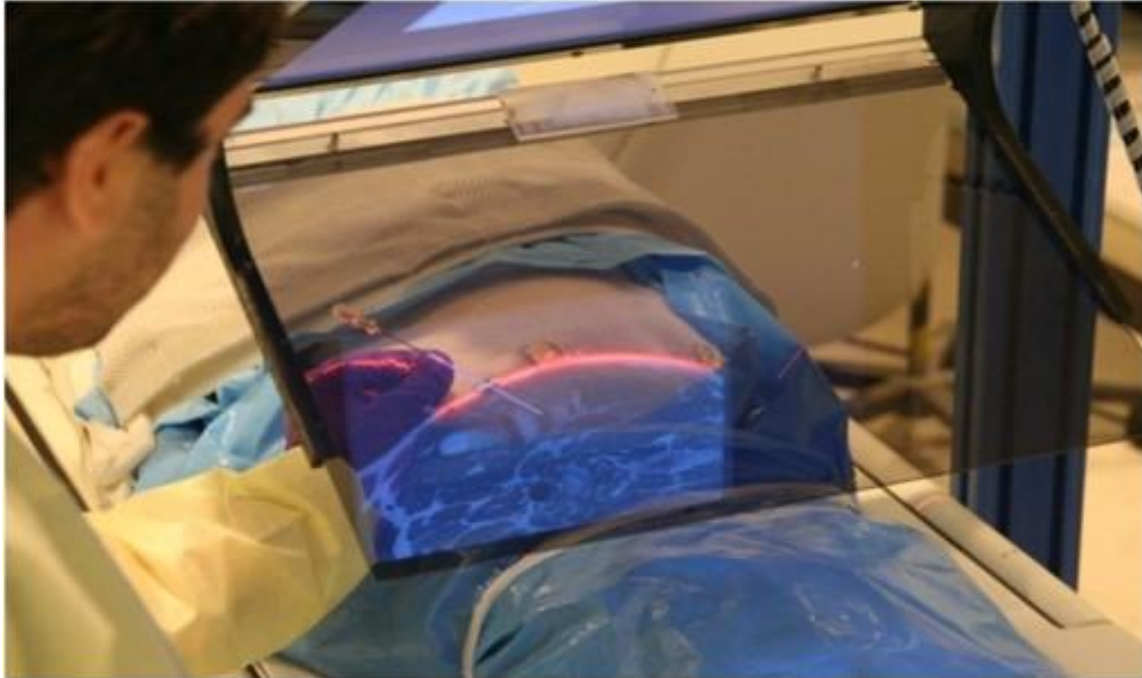


Figure 5. 2D Image Overlay System mounted to CT scanner gantry in a percutaneous needle insertion study on a simulated patient.¹⁰

The *Perk Station Training Suite* (Perk Station) emerged as a solution to many of the image overlay's issue after encouraging results were attained in validation studies [25]. It was designed and developed to aid with training clinicians and honing their skills in needle placements using AR in a range of clinical applications [26, 27]. The Perk Station was a relatively inexpensive, simple and reproducible solution for training operators in computer-assisted surgery. The Perk Station proved valuable in demonstrating the improvement in needle placement accuracy that repeated training and practice provides for a variety of clinical procedures [26, 27]. The Perk Station measured and recorded the total procedure time, time inside the phantom, path length, potential tissue damage, out-of-plane deviation and in-plane deviation for each operator and trial. In a lumbar puncture study, it was found that those who trained with Perk Station outperformed the control group with shorter path lengths, less tissue damage, and shorter procedure times [27]. There were multiple pre-

¹⁰ Unpublished image; see [23] and [24] for further details and additional images about this, and similar, systems.

clinical studies undertaken using these types of system for procedures such as shoulder and hip arthrography, lumbar spine procedures, and spine injections, which highlight the clinical relevance and importance of AR in surgical guidance [28, 29, 30].

1.4.3 Mobile CT / MRI-Based Image Overlay Systems

Mobile image overlay systems were proposed to surpass the difficulties and lack of portability that was associated with previous image overlay systems [31, 32, 33]. Mobile systems were simpler to calibrate and use in practice, as the large mounted monitors were replaced with a tablet display device. The semi-transparent glass was also affixed directly to the display. These first systems permitted handheld and wireless image overlay guidance. However; a host computer was required stemming from the lack of computational capacity in the tablet display device [31]. This led to low screen refresh rates when the system was in use, as the tablet display device was required to connect wirelessly to the host computer and mirror its screen [31].

Later designs of the mobile image overlay system encompassed a tablet computer-based mobile image overlay system with an automatic calibration process, a modular frame, all of which was packaged into a self-contained system (Figure 6) [32, 33]. This design included a calibration process which was reproducible and accurate [32]. Although this system satisfied the accuracy requirements for a range of needle interventions, its use in clinical procedures was limited by the tracking system's required floor space and surgical workflow [33].

1.4.4 Head-Mounted Video Display Systems

Some previous technologies still required clinicians to switch their view between the operation site and a computer screen. As such, the development of HMD-based surgical navigation systems started becoming increasingly prevalent [34, 35, 36]. The *Reality Augmentation for Surgical Procedure System* was one of the first AR HMDs for image-guided surgical planning and navigation [34]. Using multiple cameras, an infrared flash, and pose tracking tools, the device

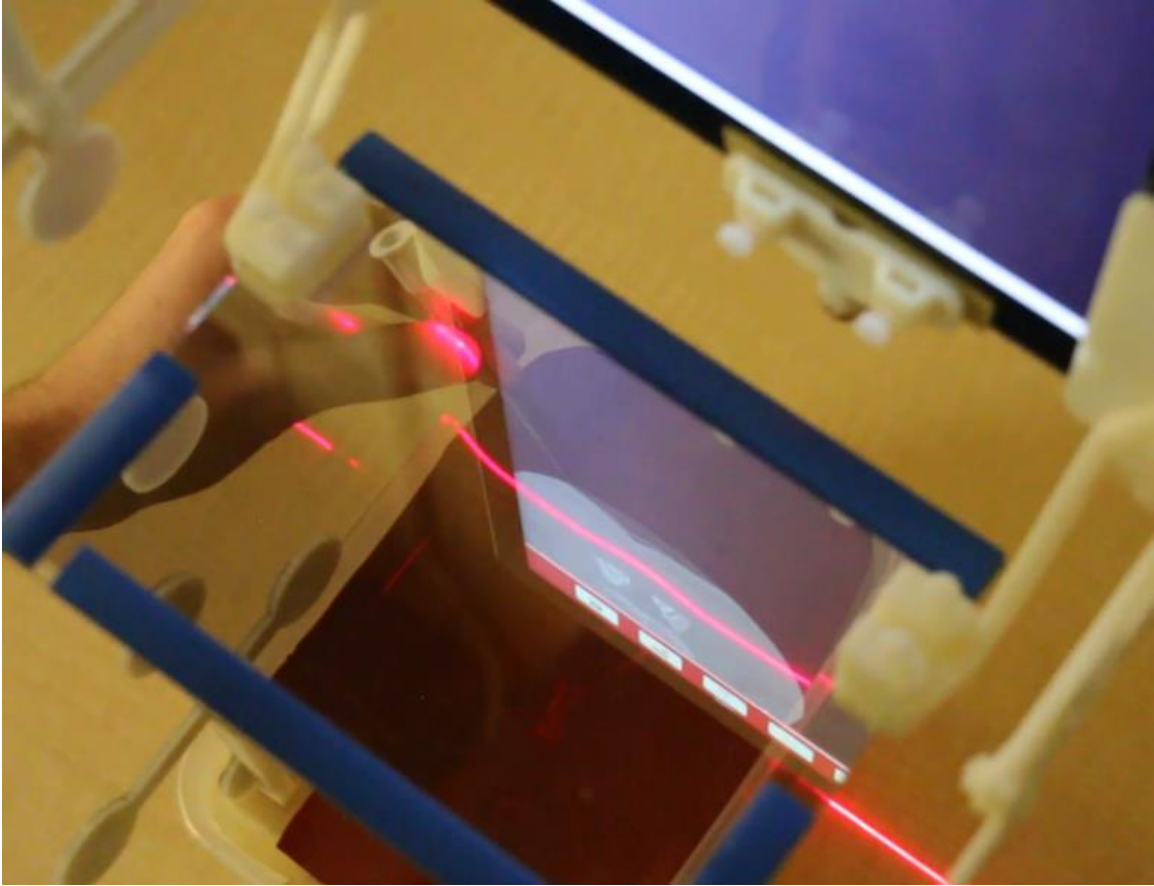


Figure 6. Mobile image overlay system prototype in use for a percutaneous needle insertion study on a phantom thoracic spine.¹¹

permitted presentation of virtual objects in a real-world environment. By designing a video see-through system rather than an optical see-through system, the system allowed more control of the resulting displayed images, at the expense of additional latencies between the real and virtual views. The camera systems allowed for no perceived lag when rendering the virtual and real images, though there was a temporal latency in the overall viewing of the images of about 100 ms [34]. By creating a device that was on the spectrum between virtual and augmented realities, Maurer *et al.* had been able to successfully take advantage of the video stream to manipulate reality, while allowing users to see their true surroundings.

¹¹ Unpublished image; see [33] for further details and additional images about this system.

1.4.5 Head-Mounted Optical Display Systems

Many subsequent systems discontinued the use of video see-through in favour of optical see-through displays as the average distance judgment of users using optical see-through displays is superior [35, 36, 37]. It has also been found that when using video see-through systems, there is a significant underestimation of virtual environment distances by the user [37].

Other systems, such as the *Augmented Reality-based Surgical Navigation System* (AR-SNS) overcame the need for introducing a temporal latency by using high-performance workstations and external optical tracking systems to render the virtual images in the correct locations relative to patient anatomy [36]. These virtual images are rendered on see-through displays which are head-mounted to give visual cues to the operator. As such, several disadvantages of traditional computer-assisted navigation systems are overcome. Most notably, the surgeon does not have to switch their gaze between the operation site and the computer screen. It has been found that the use of a HMD has no major disadvantages when compared to the conventional 'image on monitor' setup [38]. However, due to the weight and inconvenience of the HMD, the AR-SNS was deemed uncomfortable by surgeons when wearing it to conduct long procedures.

1.4.6 Navigation System Development on Commercial Platforms

Of late, light-weight and off-the-shelf AR technologies have become more abundant and available to consumers [35]. With the increase in manufacturers, technology is improving steadily and consistently in terms of portability, computational capacity, and overall usability. Multiple commercial solutions and platforms have become more readily available, and are being integrated to clinical workflows for use in image-guided surgery [35, 39, 40, 41, 42]. These systems have performed well in procedures where the target anatomy or region of interest is large and as such, the AR system's spatial mapping and optical tracking system does not require sub-millimetre accuracy [35, 41, 42]. In these types of procedures, clinicians would typically rely on the selection of patient entry points to obtain successful outcomes. Given that the acceptable target site is larger

than the accuracy of these commercial systems, the information shown to the clinician is often sufficiently accurate for clinical use [35]. As such, these light-weight head-mounted systems allowed for new questions to be asked, and for new approaches to surgical guidance and navigation to be developed.

Abhari *et al.* identified a gap between the training received for neurosurgical tumour resection and the actual practices of surgeons during operations [39]. Many available neurosurgical training tools focus on the visualization of medical images of the current case; however, spatial reference and visualization of the images *in situ* are often excluded from these training tools [39, 43]. There are many systems which incorporate immersive environments for surgical training [23, 24, 26, 27, 31], planning [23, 24] and navigation [19, 20, 21, 22] – yet these systems typically faltered by having limited user interaction due to workspace constraints or a small field of view for the operator. The mixed reality HMD proposed by Abhari *et al.* was therefore paired with an external tracking camera and custom designed software. This allowed for the accurate measurement of multiple action and perception metrics [39]. Operator performance with the use of a mixed reality planning environment was compared to the performance of operators in three other conventionally used planning environments. In their study, the participants completing tasks in the mixed reality environment demonstrated significantly lower rotational and translational errors in perception and planning activities [39]. Their system also required lower task completion times [39].

The use of ‘Smart Glasses’ and other wearable devices with heads-up displays have also recently been assessed for their applicability to surgical navigation [41]. After creating 3D models from preoperative CT or MRI images, operators were able to observe visualizations on the lenses of the glasses, and then directly in their environment by virtue of the see-through nature of the glass lenses. The glasses have passive optical tracking markers fixed to the frames so that the optical tracking system is able to report their position relative to the patient to allow the software to update visualizations in real-time [41]. As with many other tracked AR navigation systems, the clinician

had patient images and other visuals put directly into their field of view and could observe them from any angle or distance. By providing a light-weight overlay of patient images and visualizations clearly and accurately, clinicians could then navigate through patient images and models in a hands-free manner [41].

1.5 The Microsoft HoloLens

The Microsoft *HoloLens* (Microsoft Corp., Redmond, Washington, USA) mixed reality platform is considered the highest performing commercially available HMD AR platform based on its capabilities for contrast perception and frame rate [44] as well as its ergonomics [45] – among multiple other factors [44, 46]. The *HoloLens* is a fully untethered holographic computer which combines various sensors such as accelerometers, infrared lasers, microphones and cameras into a wearable headset capable of generating 3D visualizations through a reflection on to the user’s retinas, all without impeding their view of the surrounding environment. The core functionality of the *HoloLens* is achieved through the combination of two fundamental technologies. The first such technology is the projection of 3D holographic images onto the user’s eyes through pico projectors. The second being the device’s spatial mapping through Microsoft’s proprietary computer vision techniques and machine vision hardware.

Pico projectors are small hardware devices, which are also known as handheld or mobile projectors. The *HoloLens* makes use of two pico projection modules that are embedded into one module, located directly above the user’s eyes, which generates the light for the displays. This light is then transported to the “screens”, called waveguides, which direct the light to the user’s eyes.

The *HoloLens* contains six cameras, with two on the left side of the device, two on the right side of the device, and two in the center – one which contributes to the full room spatial mapping abilities, and another which is used only for capturing 2D perspectives of the room for recording and documentation purposes. These cameras provide the device with a 180-degree field of view of its

environment. The five mapping cameras are used to construct point clouds and depth representations of the environment around the device – and by extension the user. These point clouds are collected as the user moves around and are merged together and meshed to construct a representation of the environment surrounding the device. The *HoloLens* is then assumed to achieve this using a combination of methods and techniques common to solving the problem of simultaneous localization and mapping (SLAM) wherein the construction and updating of an environment are done while simultaneously keeping track of the device’s location within this environment [47]. SLAM is typically solved through an approximate solution tailored to the resources of the system [48]. Unfortunately, the implementation and methods used on the *HoloLens* are proprietary knowledge of Microsoft and are not publicly known.

1.5.1 Surgical Guidance and Planning with the Microsoft HoloLens

The proposed systems which were described previously (See 1.4.6 Navigation System Development on Commercial Platforms) by Abhari *et al.* and Maruyama *et al.* occupied large footprints – requiring external tracking systems and host computers to render the displayed data [39, 41]. With HMD systems narrowing the gap between low-cost and practicality, the *HoloLens* takes this a step further and aims to bring light-weight, portable, low-cost, and practical surgical navigation (Figure 7) and surgical training (Figure 8) to the operating room and simulated study.

Several research groups have been working to create systems on the *HoloLens* platform which are usable for AR surgical guidance, planning, and learning in an intraoperative or bedside clinical environment across various medical domains [40, 42, 44]. Recently, there has been continued development of 3D holographic tools and features that allow for surgical planning, navigation and training with hand-gestures, voice-commands, and the use of external input devices – such as wireless keyboards, mice, or other hand-held controllers.



Figure 7. The *HoloLens* used for insertion of a catheter in an extraventricular drain.¹²



Figure 8. The *HoloLens* as part of the *VimedixAR* simulated ultrasound medical training system.¹³

¹² Andrew Cutler (Duke University), *Neurosurgery resident Andrew Cutler demonstrates how HoloLens-aided EVD placement might look when performed in a clinic or ER*, accessed March 1 2019, <https://today.duke.edu/2016/10/brain-surgery-may-get-bit-easier-augmented-reality>

¹³ CAE Healthcare, *VimedixAR with HoloLens*, accessed 1 March 2019, <https://caehealthcare.com/ultrasound-simulation/vimedix/>

Morales *et al.* developed tools for visualization of MRI images on the *HoloLens* [40]. These tools and software allowed users to view, browse, and manipulate registered image slices on the patients, as well as adjust the brightness levels and contrast windows [40]. Adjusting contrast and brightness with voice-commands proves useful, as these adjustments are a standard task which is performed daily in real clinical practice for surgical planning and navigation. Providing this hands-free interaction with medical images for surgical planning may prove useful in the day-to-day tasks of clinicians. Additionally, the tools which were developed allowed users to virtually navigate through brain vasculatures [40]. Planning intravascular interventions through virtual navigation is not currently done in clinical practice. However, clinical standards in the future may involve clinicians making use of interactive and increasingly virtual planning methods [40].

Rae *et al.* assessed and investigated the use of holographic models displayed on the *HoloLens* for localization of burr holes in craniostomy procedures. In these procedures, clinicians would typically use a drill bit which is 4 mm in diameter, with the aim of successfully identifying the location of the drill entry point within a clinically acceptable range of 10 mm of the pre-planned target, in this case, a subdural hematoma [42]. To assess the feasibility of using the *HoloLens* for planning the drill location in craniostomy procedures, multiple users registered models to a simulated patient. Inexperienced users were able to place 98% of markers within the clinically acceptable range and experienced users were able to place all markers within the clinically acceptable range [42]. Additional testing was performed on simulated patients with hair to ensure the registration process could be completed accurately without relying on the curvature of the skull. In these tests, inexperienced users were able to place 96% of markers within the clinically acceptable range, and experienced users were able to place all markers within the clinically acceptable range [42].

These results were promising, suggesting that the *HoloLens* may be feasible for use in target localization in surgical planning and for surgical guidance. It was also found that with experience, the quality of the registration increased [42]. However, the results obtained by inexperienced users

suggest that it does not take much practice or difficulty to become experienced in and capable of using virtual or holographic tools for surgical planning and navigation.

1.6 Clinical Motivation

Neurosurgery encompasses a variety of different procedures, all of which vary in their use of intra-operative imaging. Subdural hemorrhage evacuations, brain tumour resections or biopsies, ventriculostomies, and many other procedures require intracranial access through burr holes.

Chronic subdural hemorrhages are usually attributed to head trauma in older individuals [49], though the estimated incidence is between 3-15.5 per 100,000 people in the general population [50]. However, this number rises when looking only at older individuals, with incidence rates of 58 per 100,000 for those 65 years of age and above [49]. Subdural hemorrhages are commonly treated with the placement of a drain through a burr hole, where surgeons drill a hole through the patient's skull commonly using either standard or roughly estimated locations.

Brain tumours are a commonly encountered neurosurgical condition that has risen in prevalence over the past several decades, with an incidence rate for primary brain tumours in the United States of 14.4 per 100,000 persons [51]. The course of treatment for brain tumours varies with the grade and location of the tumour, however, when appropriate, surgical interventions are used to resect the patient's tumour. Resections are generally performed using a craniotomy, where a piece of the skull, called a bone flap, is removed to allow access to the brain. Bone flaps are typically removed using a drill and a specialized tool called a craniotome.

External ventricular drains are commonly inserted into the brain using a freehand technique where the desired drill location is determined using surface landmarks and is highly dependent on surgeon expertise and knowledge. This type of implantation typically carries a 13–19% risk of shunt misplacement with non-functional drainage [52] and a 5% risk of hemorrhage or injury to eloquent brain [53].

In some cases of each of these various types of procedures, the anatomical targets, such as a tumour, hemorrhage or enlarged ventricle, are easily identified in the patient's images by the neurosurgeon. In procedures where the target is easily identifiable, neurosurgeons begin by planning and identifying the optimal entry point to place a burr hole and the appropriate trajectory to the lesion in order to minimize the size of the skull opening while avoiding critical structures. The ability to plan and identify the optimal drill location and drill angle of a burr hole for a given procedure is a fundamental element of a neurosurgeon's skillset and a core piece of the neurosurgical training curriculum. Assuming that the target anatomy is clearly enhanced in the patient's imaging, the principal challenge for a neurosurgeon is to mentally transfer their planned drill path from what they can see in the patient's images to the physical patient.

As such, some procedures have become increasingly reliant on the use of medical imaging and technologies, like those previously discussed in this chapter, as a tool for determining pre-operative plans and intra-operative guidance to improve surgical outcomes and reduce patient morbidity. In some cases, neuronavigation systems can help to determine drill location and drill angle [54]. However, these methods still rely on a surgeon's ability to interpret, reconstruct and visualize 2D medical images into 3D [46, 55, 56, 57]. These tasks are difficult and rely heavily on surgical knowledge, experience, and spatial reasoning skills.

1.7 Augmented Reality in Neurosurgery

As was previously discussed in this chapter, there are many enabling technologies for AR which have been proposed that may add value to neurosurgical planning, guidance and training. In addition to the methods presented earlier, AR images have already been coupled with other real data sources such as hand-held cameras, endoscopes, fluoroscopy [57], through an operating microscope [58], or even displayed over a movable tablet computer [59] in various neurosurgical contexts.

AR technologies have already been used in neurosurgery to aid in the visualization of lesions [58, 60], hemorrhages [61] and hydrocephalus [57, 62]. Additionally, AR technologies which manifest in the form of HMD have been shown to be beneficial for surgical planning and visualization [34, 39, 57, 63, 64]. As such, AR and HMD technologies are well positioned to address the problems of reliance on surgical knowledge and spatial reasoning skills given their ability to display three-dimensional (3D) anatomical models, imaging, information, and other surgical data aligned with the patient and in the user's view. More recently, the *HoloLens* has been used to provide hands-free holographic visualizations in various neurosurgical applications [40, 65, 66, 67].

AR has the potential to benefit and improve current surgical and neurosurgical practice, but prospective and clinical feasibility studies, as well as application studies, have been limited [68]. AR has yet to see routine or wide-spread success as ideal applications have not yet been widely demonstrated. Whether its use provides improved outcomes remains unclear [67], as studies to demonstrate the effectiveness of AR in training and clinical scenarios are still needed [69].

1.8 Competency-Based Medical Education

Of late, medical education has been moving towards the model of competency-based medical education (CBME). CBME allows trainees to progress through given curricula at their own pace, and to proceed past the current curriculum once they have demonstrated competency in specific, objective benchmarks and metrics [70].

Previously, residency programs were time-based and required trainees to spend one full year at a given level or Postgraduate Year before proceeding. CBME does not focus on the amount of time spent for determining promotion through the program but on the trainee's demonstration of competence. CBME-based programs are typically structured in four different stages; i) 'transition to discipline', ii) 'foundation of discipline', iii) 'core of discipline' and iv) 'transition to practice' [71]. In each stage, trainees will focus on different tasks. In the first stage – 'transition to discipline',

the focus is concentrated on orienting the trainee to the new environment and showcasing what comes next. As they progress into the second and third stages – ‘foundation of discipline’ and ‘core of discipline’, trainees will be focused on the foundational and core skills that are required for achieving overall competency in the field and in their desired discipline. Finally, in the fourth stage – ‘transition to practice’, trainees demonstrate their ability to practice their discipline and learned skills autonomously.

Furthermore, there are several benefits to medical education and the CBME model provides. Trainees will receive increased levels of supervision, assessment, and mentorship [70]. This will ensure that competencies and expertise are being demonstrated by trainees in each stage of the program [72]. Trainees who are able to demonstrate competency at higher rates may be given the option to pursue additional opportunities for enrichment. As such, instead of finishing their program earlier, these trainees will be given additional time to work on other materials of interest through electives or in research.

The CBME model ensures that trainees who have not reached competency cannot provide care without supervision in a clinical setting and during their interactions with patients. The shift towards CBME will help the next generation of physicians become better healthcare providers, and will provide a better educational experience for those involved. Through individualized learning, increased flexibility, the inclusion of new and innovative assessment methods, and the ability to give meaningful feedback during increasingly frequent assessments; CBME will prepare trainees for practice more effectively [70].

1.8.1 Neurosurgical Residency Programs

Currently, neurosurgical trainees learn these planning and spatial reasoning skills through observerships and apprenticeships inside and outside of the operating room for approximately 6-8 years after completing medical school. Much of this training is complex, hands-on, and leaves trainees able to acquire fundamental skills only when specific procedures occur in a clinical context.

One of the challenges associated with CBME, especially in surgical disciplines, is the need for ongoing tracking of an individual's learning curve through objective measure as they progress towards competency [72]. Recently, to ensure compliance with CBME, there has been a shift towards methods for quantitative assessment of skills, often using position tracking, as this does not require direct expert supervision [73].

However, in addition to the difficulties in tracking progress, there is a lack of demonstrated neurosurgical performance metrics which translate to successful patient and surgical outcomes in practice and are usable for providing trainees with any meaningful feedback. This leaves trainees unable to train or develop skills, such as planning and identifying optimal drill locations and drill angles on simulated or real patients, on their own time. As such, a neurosurgical curriculum which follows the CBME model may prove principally important for the training and skill development of future neurosurgical trainees. Practice with simulation-based training platforms in other surgical specialties has been heralded as an effective learning strategy [68] and has been thought to be the next step for neurosurgical training curricula [74].

1.9 Objective

This work sought to determine relevant, valid, objective, and transparent performance metrics which are CBME compliant and are usable for differentiating between novices and experts. Next, these metrics were used to determine whether the use of AR adds practical value to teaching and planning of neurosurgical procedures. By comparing the use of AR to standard practice in three common and motivating neurosurgical procedures – drainage of chronic subdural hemorrhage, brain tumour resection, and insertion of external ventricular drains – that vary in their use of image-guidance, the utility of AR was assessed in trainees and surgeons to determine the role of expertise in this technology.

1.10 Contributions

The main contributions of this thesis are:

- The design and implementation of an AR application and platform for intra-operative guidance for planning and localizing optimal drill locations and drill angles in neurosurgery;
- An intra-operative performance study to compare the benefit of AR for surgical planning to conventional methods for trainees and attending neurosurgeons;
- A simulated-environment training study wherein trainees demonstrated their ability to identify optimal drill location and drill angle in space using our AR application, as well as two other conventional visualization methods.

In Chapter 2, contributions regarding the design and implementation of the AR application are described. The testing and validation of all developed software for the application is described and all results are presented.

In Chapter 3, the intra-operative performance study is described. In this chapter, the study and experimental design are discussed. Through this study, the validity of the developed metrics for assessing performance in localizing optimal drill location and drill angle is assessed. Here, the metrics are also validated for their use in differentiating between trainees and attending neurosurgeons in that same task.

In Chapter 4, the simulated environment training study is described. Here, the experimental design and results, wherein it was sought to prove if displaying optimal surgical plans could significantly aid users in identifying optimal drill locations and drill angles on simulated patients.

Chapter 2

System Design and Implementation

2.1 Software Implementation

The *HoloLensQuickNav*¹⁴ (*HoloQuickNav*) software was initially designed within the Laboratory for Percutaneous Surgery, as an application to be used for intraoperative AR planning in neurosurgical procedures using the *HoloLens* [42]. *HoloQuickNav* was developed using the cross-platform Unity engine (version 2018.1.0f2) for AR and virtual reality software. Multiple components from Microsoft's open-source and cross-platform Mixed Reality Toolkit¹⁵ were incorporated into the application in order to accelerate development. All other remaining components and code were created specifically for *HoloQuickNav*.

To navigate menus, load models, register the holographic images and to control other aspects of the application, an *Xbox One Wireless Controller* (Microsoft Corp., Redmond, Washington, USA) was incorporated into the system as a handheld controller for the application. A handheld controller was selected for use with the software as previous work with voice commands and *HoloLens* 'AirTap' gestures did not provide enough flexibility and ease of use with *HoloQuickNav* [42]. Several of the core components, including file loading and patient model visualization, were inherited from previous versions of the software and incorporated into an updated version of the software for the contents of this work. The Patient Manager (Section 2.2 Model Creation and Visualization) and controller-based registration method (2.3 Registration Method), described below, are new for this work.

¹⁴ *HoloLensQuickNav*, <https://github.com/PerkLab/HololensQuickNav>

¹⁵ *MixedRealityToolkit*, <https://github.com/Microsoft/MixedRealityToolkit-Unity>

2.2 Model Creation and Visualization

Anatomical models of a patient's skin surface, brain, and intra-cortical lesion can be generated from either MRI or CT images using *3D Slicer*'s Segmentation and Surface Toolbox modules [14]. Once exported as a Wavefront .obj (OBJ) file for use on the *HoloLens*, *HoloQuickNav*'s application's Patient Manager displays a list of all sets of anatomical models which are available on the *HoloLens* once they have been stored on the device as OBJ files (Figure 9). In addition to storing the models as OBJ files, an eXtensible Markup Language (XML) file was created and stored on the *HoloLens* for each set of OBJ files. XML is a self-descriptive file format used for storing and transporting data. Its use with the application allows to the software to programmatically determine all files which are stored on the *HoloLens*'s local storage that are associated with a given study by providing the file paths and names for each required model in the view to be displayed.

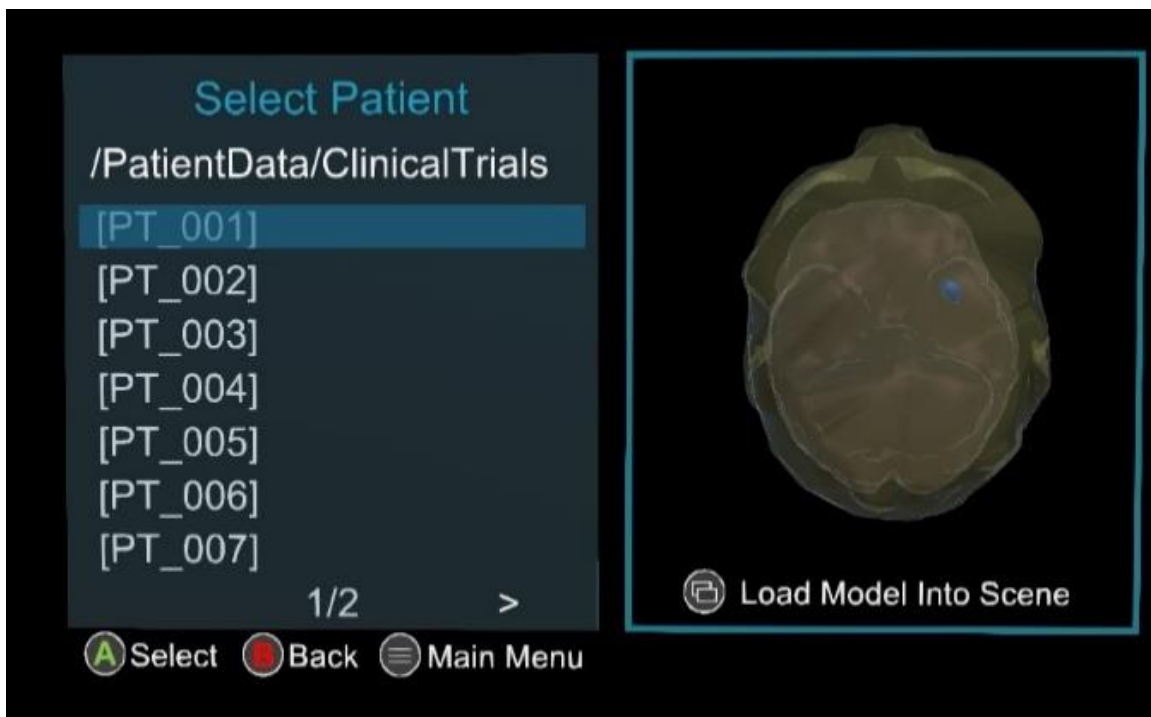


Figure 9. *HoloQuickNav*'s Patient Manager showing a preview of all models on the device. This image shows the skin surface, brain, and intra-cortical lesion models. This image was captured with the real-world environment removed from all images to better visualize the user interface.

2.3 Registration Method

Once loaded (Figure 10), *HoloQuickNav* allows users to manually register holographic models to the phantom by translating and rotating the models using the handheld controller's thumb-sticks (Figure 11a). Users are able to translate or rotate the holographic model interchangeably in each direction or about a chosen axis. Once the user is satisfied with the result, they can 'lock' the registered holographic models in place (Figure 11b). With the registration process complete, the user can adjust which models are visible in their view. This allows the visibility of the skin, brain, intra-cortical lesion, and any surgical plans or annotations to be set independently.

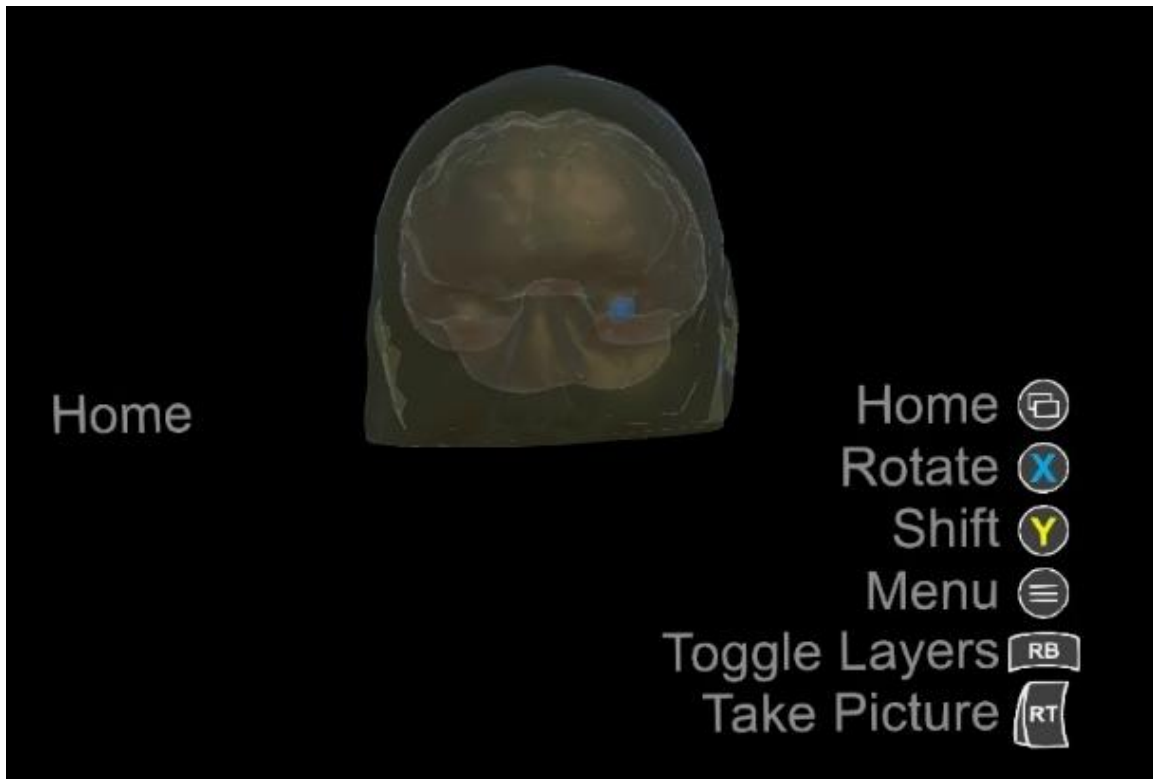


Figure 10. *HoloQuickNav*'s main user interface when registering the models to the patient. This image shows the skin surface, brain, and intra-cortical lesion models. This image was captured with the real-world environment removed from all images to better visualize the user interface.

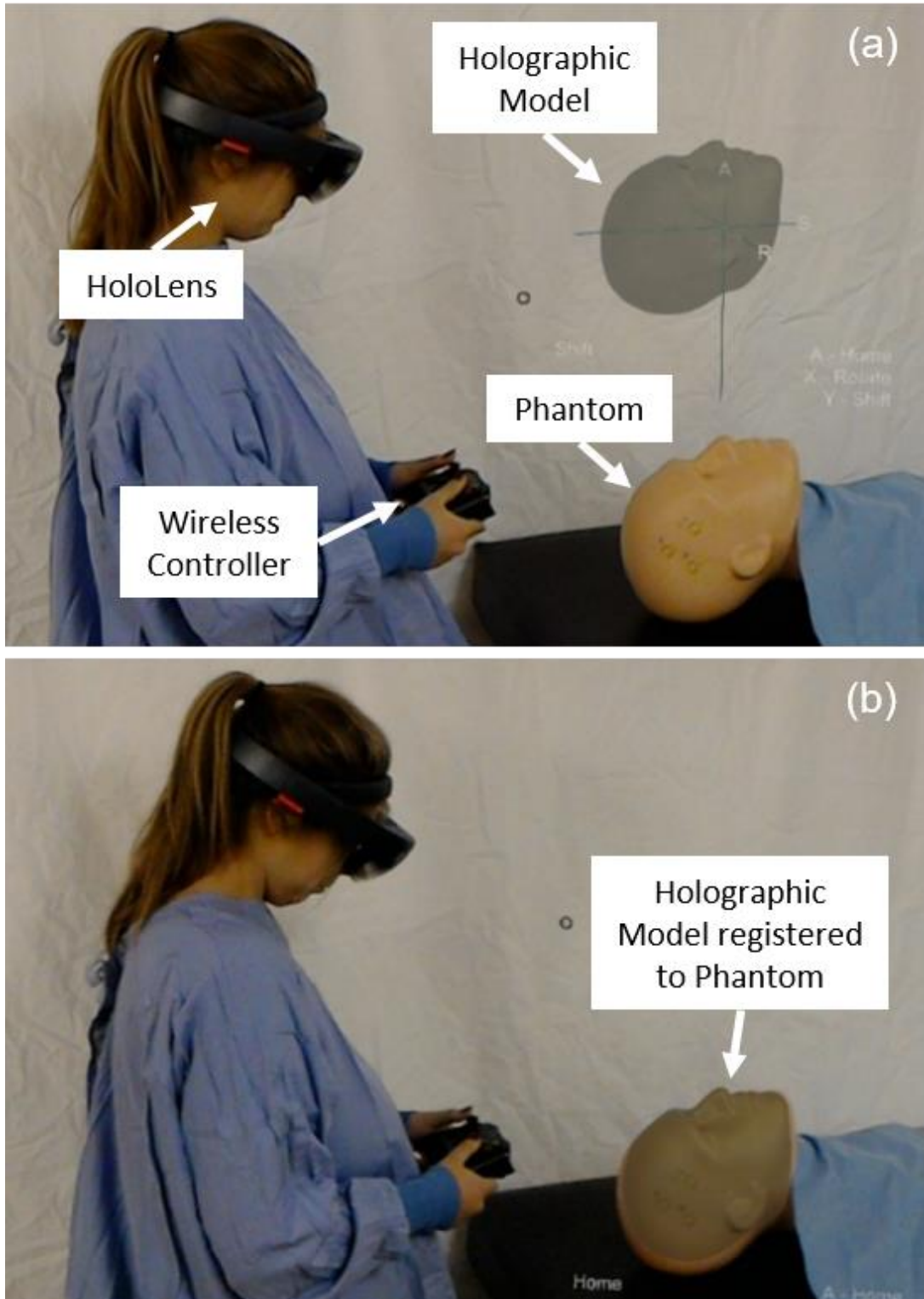


Figure 11. The registration process for *HoloQuickNav* with (a) the user translating models towards the simulated patient and (b) models in place on the simulated patient relative to the user.

2.4 Registration Accuracy and Feasibility Study

A pair of plastic male and female phantoms were used to assess the accuracy of the registration method. A series of three 2 mm diameter steel ball bearings were affixed to each phantom on the right medial surface as reference markers. Each reference marker was used to assess the registration accuracy at a given point on the phantom. A CT scan was acquired of each phantom with the ball bearings affixed to it, and all models were created for each phantom to be used with *HoloQuickNav*.

The registration of holographic models to each phantom was completed by 13 different participants. Ten participants were considered novices as they had little or no previous experience with *HoloQuickNav* or HMD AR technologies. Three participants were considered experts as they had a high level of experience with the application or were familiar with HMD AR technologies, such as the *HoloLens*. Prior to commencing the study, participants were briefed and given a demonstration on how to use *HoloQuickNav*. Participants were given five minutes to practice using the *HoloQuickNav* and to learn to use the controls required to register holographic models to the phantom. No participants required the full five minutes of practice to become comfortable with the *HoloQuickNav*.

Participants attempted three registrations on four phantom types, for a total of 12 registrations, over two separate sessions. Registrations were completed on a male phantom with and without hair, and a female phantom with and without hair (Figure 12). In the first session, participants completed six registrations. In a second session, 24 – 48 hours later, participants completed the remaining six registrations. The order in which participants completed registrations was randomized.

Participants started the registration process from a predefined location 0.75 away from the phantom, standing straight and comfortably, facing forwards with their head pointed directly towards the phantom. While participants were encouraged to move around the space in order to visualize and view the holographic models from multiple angles while completing the registration process, before finishing each registration, participants were asked to return to the pre-defined starting position.

This was done to ensure that all registrations were completed at the same distance from the phantom, and that all reported accuracies were acquired from the same position. The distance from the phantom distance was defined as such as when used intra-operatively, it is beneficial for clinicians to be able to be at close proximity to the patient when using the technology, but not so close as to be within the minimum distance for virtual objects for the *HoloLens*. Microsoft recommends a minimum clipping render distance of 0.85 m, and suggests that holographic models be viewed between 1.25-5 m. However, it has been reported that in applications where holographic models and the user are stationary, objects can be viewed from as close as 0.5 m¹⁶.

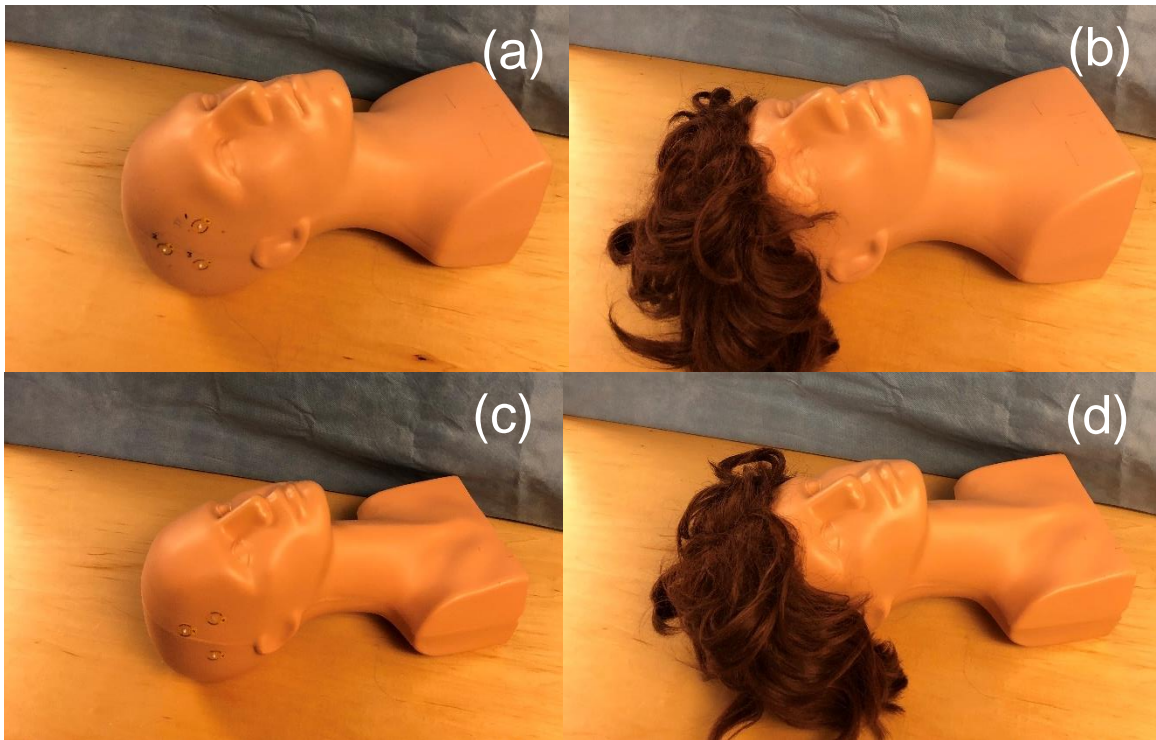


Figure 12. The male plastic phantom (a) without hair and (b) with hair and the female plastic phantom (c) without hair and (d) with hair.

Following each registration, red markers were revealed on the holographic skin surface model to indicate the location of the ball bearings. Participants self-reported the range in which each red

¹⁶ Microsoft Corp., *Hologram Stability*, accessed June 19 2018, <https://docs.microsoft.com/en-us/windows/mixed-reality/hologram-stability>

marker was located from each of the ball bearings, using the guide shown in Figure 13. Self-reporting was required as no camera or external sources are able to see exactly what the participants are able to when wearing the *HoloLens*. The amount of time required for each participant to complete each registration was also recorded.

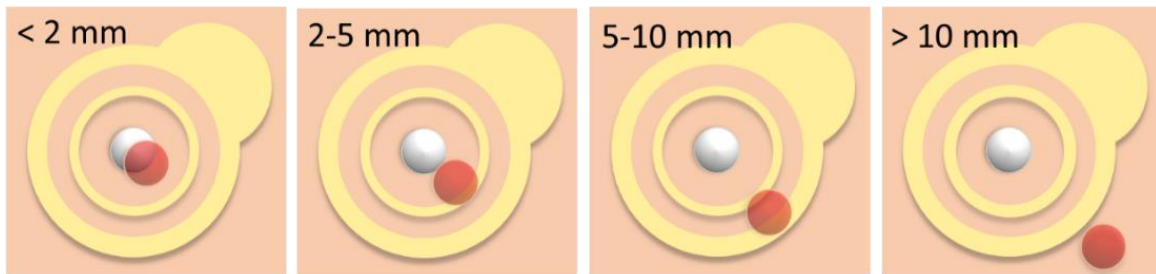


Figure 13. Different ranges of accuracy for self-reported holographic marker placement by users in the registration accuracy and feasibility study.

2.5 Results and Discussion

Registration accuracies for novice ($n = 10$ users, $n = 120$ total registrations) and expert ($n = 3$ users, $n = 36$ total registrations) users are presented in Table 1 and Figure 14. Times taken to complete the registrations for novice and expert users are presented in

Table 2 and Figure 14.

A two-tailed Mann-Whitney U Test for independent unpaired samples demonstrated a significant reduction in the time taken by experts relative to novices ($p < 0.001$) to complete registration tasks.

These results reveal the variability, and the lack thereof, in the ability of users of all experience levels to properly register the holographic models based solely on surface features of a plastic phantom. Additionally, given the smaller size and therefore less curved surface of the female phantom's head, it is possible that users encountered a more difficult task when attempting to accurately register the holographic models to that phantom. Though the registrations that were within the acceptable range were comparable, the amount of registrations that into the less accurate categories were higher (Figure 15).

Table 1. Registration accuracy results.

Group	Phantom Type	< 2 mm	2–5 mm	5–10 mm	> 10 mm	Within Range
Novice (n = 10)	Male	10%	29%	57%	4%	96%
	Male (hair)	8%	40%	45%	7%	93%
	Female	9%	27%	63%	1%	99%
	Female (hair)	3%	16%	71%	10%	90%
	<i>All</i>	7%	28%	59%	6%	94%
Expert (n = 3)	Male	40%	30%	30%	0%	100%
	Male (hair)	33%	56%	11%	0%	100%
	Female	15%	25%	49%	11%	89%
	Female (hair)	15%	44%	41%	0%	100%
	<i>All</i>	26%	39%	32%	3%	97%
All	All	12%	30%	53%	5%	95%

Table 2. Registration task completion times.

Group	Phantom Type	Min. Time [s]	Max. Time [s]	Mean Time [s]
Novice (n = 10)	Male	46	315	137
	Male (hair)	58	364	119
	Female	52	307	133
	Female (hair)	58	206	119
	<i>All</i>	46	364	127
Expert (n = 3)	Male	31	125	72
	Male (hair)	35	111	68
	Female	25	119	82
	Female (hair)	36	92	65
	<i>All</i>	25	125	72
All	All	25	364	114

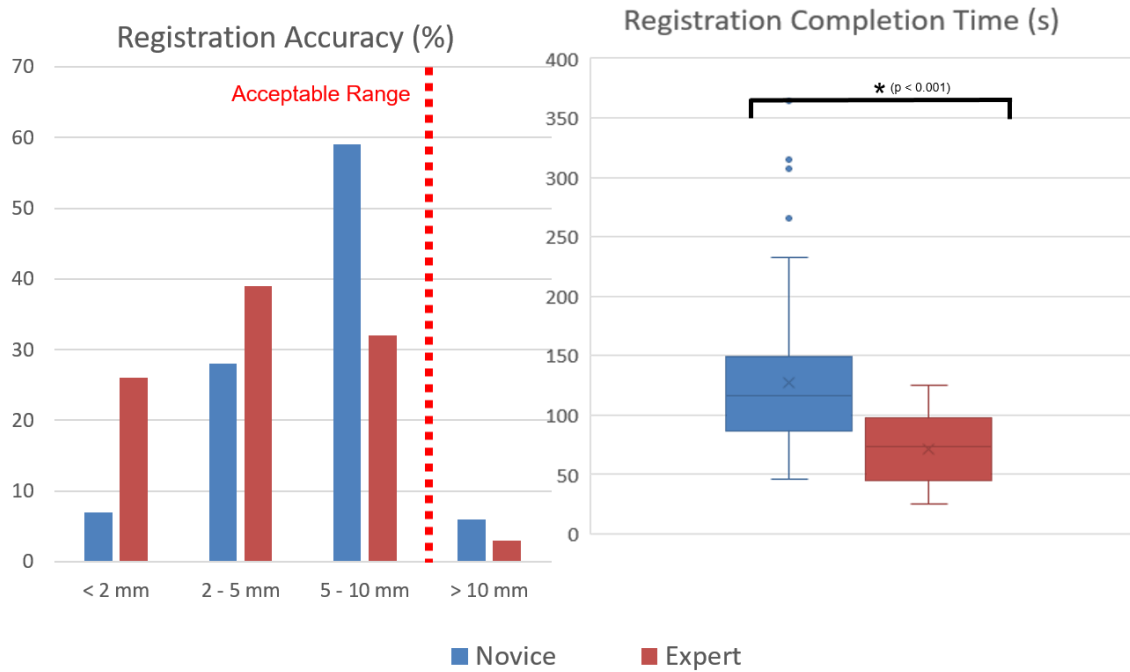


Figure 14. Bar chart assessment of all registration accuracies (left) and box and whisker plot of all registration times (right) for novice and expert participants.

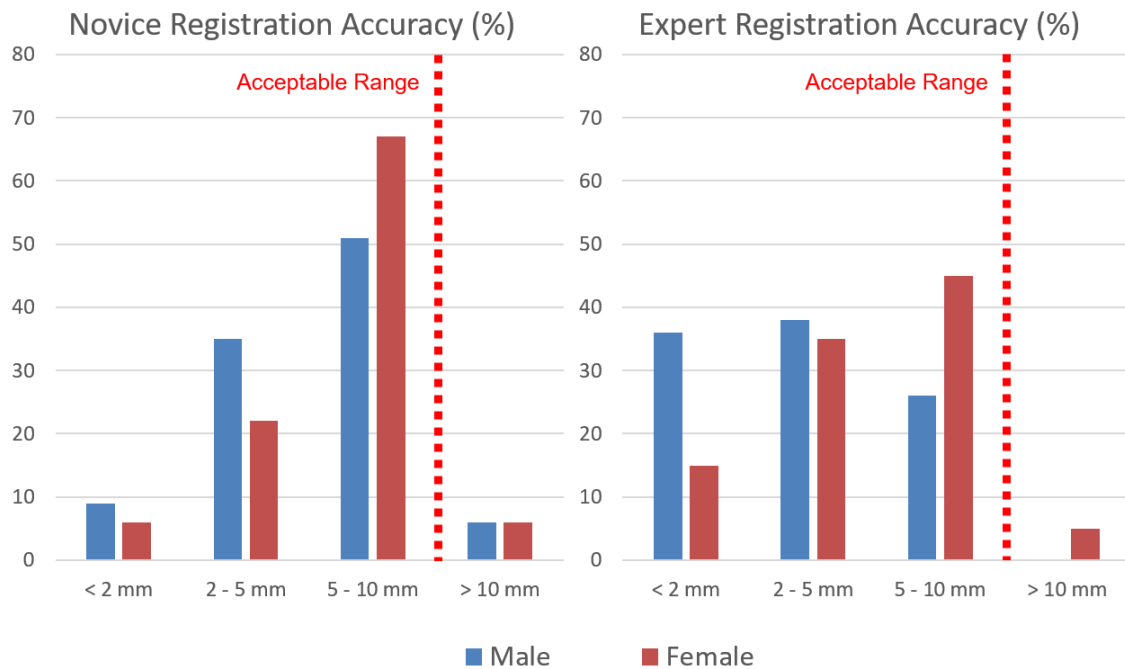


Figure 15. Bar chart assessment comparing male and female phantom registration accuracies for novices (left) and experts (right).

Novice users were able to register the holographic models within the predefined acceptable range of 10 mm 94% of the time, while expert users were able to do the same 97% of the time. These results may indicate that the advantage of increased experience with the registration process and familiarity with the control scheme reduces the time taken to complete a registration. The range in registration times taken by novice users in the study (46-364 s) appears consistent with values reported in the literature. Rae *et al.* reported times between 135-219 s [42] and Frantz *et al.* reported times between 51-165 s [66]. However, this method shows an overall faster and less varied range of time (25-125 s) for expert users [42, 66]. These methods may also be applicable for registration tasks in other types of surgery, as manual registration methods based on aligning surface features have previously been trialled intra-operatively in extremity reconstruction surgery and observed similar registration times with a reported range of 60-120 s [75]. However, while the registration times obtained in this registration study by expert users are lower than most reported values in the literature, it is possible that these results may be attributed to not only the control scheme that was developed but to the level of user experience with this software or the familiarity with AR technologies.

2.6 Summary

This chapter has presented the methodology for design, implementation and preliminary feasibility testing of an AR application, *HoloQuickNav*, for intra-operative guidance and planning in neurosurgery. This application includes functionality for automatic management of patient models for display intra-operatively or in a simulated training environment. Additionally, it includes functionality for performing a manual registration to overlap the holographic models with the patient, be it simulated or real.

Thorough testing and validation were conducted to ensure that our application is sufficiently accurate and feasible for intra-operative use. This was done by ensuring that our registration method was able to consistently be performed in a timely manner while achieving the required level of

accuracy. These validations confirmed that our method was able to meet the required levels of accuracy for a manual registration in a time which was comparable, if not faster to what has been seen in the literature.

Chapter 3

Intra-operative Planning and Target Localization

3.1 Study Design

The intra-operative planning and target localization study was conducted as a prospective cohort study. The study was approved by the Queen's University Health Sciences and Affiliated Teaching Hospitals Research Ethics Board (see Appendix A, Appendix B). Voluntary enrollment and signed consent were obtained prior to each procedure from patient subjects as well as from each attending neurosurgeon and trainee participant. Clinical feasibility of the *HoloQuickNav* system and software was tested in an operating room environment with human patients. This work sought to assess whether the use of *HoloQuickNav* better informs surgeons and trainees in their localization of optimal drill location and drill angle for neurosurgical procedures through an intraoperative performance comparison. Additionally, it was sought to validate if the developed metrics were usable for differentiating between trainee and attending neurosurgeon performance in the localization of optimal drill location and drill angle.

3.2 Study Participants and Setting

Medical students and medical student clerks, general surgery residents, and attending neurosurgeons were recruited from the Queen's University School of Medicine, Queen's University General Surgery residency program and Kingston General Hospital Department of Surgery, respectively. The medical students and residents were considered trainees for this study. Neurosurgical trainee and attending neurosurgeon outcomes were considered separately in the study as knowledge expectation in their neurosurgical planning experience differs.

The participants performed the study in an operating room once the patient was anesthetized, and prior to the patient being draped or the surgery commenced. I was present to facilitate the study and answer technical questions about the use of the AR visualization tools; however, questions

related to surgical planning, and localization of optimal drill locations or drill angles were not answered during the study.

3.3 Study Protocol

Fifteen cases which underwent intracranial surgical intervention for drainage of chronic subdural hemorrhage, brain tumour resection, or insertion of an external ventricular drain at Kingston General Hospital in 2018 were included in this study. Of the 15 cases, 13 were patients with primary or secondary brain tumour, one was a patient with subdural hemorrhage, and one was a patient with hydrocephalus.

Inclusion criteria for all cases required that the subject's age was greater than or equal to 18 years old, the subject was able to give informed consent, and the subject was diagnosed with i) a brain tumour and will undergo surgical resection of the tumour, ii) a subdural hemorrhage and will undergo a surgical intervention, or iii) hydrocephalus and will undergo a surgical intervention. Cases were excluded from the study if i) the subject had undergone previous intracranial surgery, ii) the patient subject was undergoing an immediate or within 8-hour emergency intervention, or iii) the patient subject was unable to provide informed consent.

Preoperative patient CT or MRI images were used to provide the visualizations for surgical planning. All Digital Imaging and Communications in Medicine (DICOM) data was imported into a workstation having previously been anonymized and with all identifying patient data removed. DICOM is the standard for the communication and management of medical imaging information and its related data. Patient images were reviewed by experienced technicians and attending neurosurgeons to provide expert opinions on the image segmentations, which, in turn, became the resulting holographic models that would be displayed through the HMD to the participants during the intra-operative study.

Each case had the attending neurosurgeon and trainee plan their procedure using a conventional 2D method and an AR method while in the operating room. The 2D method had the participant denote the location of the lesion and the trajectory using a pointer tool, with a series of 2D images available for reference. The AR method had the participant denote the location of the lesion and the trajectory using a pointer tool while wearing a *HoloLens* running *HoloQuickNav*. The 2D method required participants to use the preoperative patient CT or MRI images alone to plan the location and trajectory at which they would create a burr hole. The AR method allowed participants to use and view holographic models of the surface anatomy and intra-cortical lesion virtually floating over the patient to plan the location and trajectory at which they would create a burr hole.

Prior to using the AR method in the operating room, participants were shown how to use the technology and perform a registration with the handheld controller through a sample case. This case allowed them to learn how to interpret and manipulate the holographic models. During this sample case, it was explained to the trainees and attending neurosurgeons that they should report drill locations and drill angles which were the intended path of the catheter in subdural hemorrhages and hydrocephalus, or the in the direction of the desired center of the craniotomy for the brain tumour.

3.4 Experimental Design

Once the patient was brought into the operating room, they were anesthetized and positioned for surgery. The trainee used the 2D method to identify the lesion and trajectory. The pointer was oriented along the desired trajectory while several coloured 3D point clouds of the scene were acquired using the *Intel RealSense D415 Depth Camera* (Intel Corp., Santa Clara, California., USA) to determine the drill location and drill angle which were identified by the trainee. Next, the attending neurosurgeon used the 2D method to identify the lesion and trajectory. Point clouds of the scene were acquired to quantify the attending neurosurgeon's planned drill location and drill angle using the 2D method. I then registered the holographic models to the patient, before allowing the trainee or attending neurosurgeon to complete the process before denoting their drill location

and drill angle (Figure 16). The trainee then used the AR method to identify the lesion and trajectory (Figure 17). Point clouds were acquired of the trainee's planned drill location and drill angle using the AR method. Next, the attending neurosurgeon used the AR method to identify the lesion and trajectory (Figure 18). Point clouds were acquired of the attending neurosurgeon's planned drill location and drill angle using the AR method.



Figure 16. Neurosurgeon using the *Xbox One Wireless Controller* while wearing the *HoloLens* to register the holographic models to a patient.

Lastly, the neuronavigation system was registered to the patient. The attending neurosurgeon used a frameless neuronavigation system, such as the *NAV3i* (Stryker Corp., Kalamazoo, Michigan, USA) or *Brain Lab VectorVision* (Brainlab, Munich, Germany), to identify an optimal drill location



Figure 17. Trainee (right) using the pointer to indicate the drill location and drill angle while wearing the *HoloLens* as a 3D point cloud of the scene is acquired using the *Intel RealSense D415 Depth Camera* (left).



Figure 18. Neurosurgeon (right) using the *HoloLens* to denote the surgical access point and trajectory before commencing surgery.

and drill angle. Point clouds are acquired of the attending neurosurgeon's planned drill location and drill angle using the standard neuronavigation system. This drill location and drill angle were used as the clinical gold-standard. Should neuronavigation not be used for the surgery, the attending neurosurgeon's drill location and drill angle with the 2D method was defined as the clinical gold-standard.

3.5 Data Processing

To process the acquired 3D point clouds of the surgical scene, each point cloud was opened in *MeshLab* (ISTI-CNR Research Center, Pisa, Italy), a 3D mesh processing software system for processing, editing and cleaning large unstructured meshes. Each of the individual point clouds was first rendered as a mesh and subsequently filtered to remove extraneous and irrelevant points such as those from the operating room's walls and floor, or any other objects not relevant to the patient's head and the pointer.

Once all captured 3D point clouds had been converted into a mesh and had been filtered appropriately, each mesh was registered to one another using *MeshLab*'s Align tool to allow for the chosen drill location and drill angle to be determined programmatically. The Align tool allows the user to perform a 'Point Based Glueing' wherein a series of four or more points are defined manually to roughly align features on the different meshes. Once an initial 'Point Based Glueing' has been performed, the Align tool allows users to perform an iterative closest point (ICP) registration. This registration was performed using only the facial features in the mesh, and with any surgical equipment, the pointer tool, or participant hands excluded. A sample of an aligned series of meshes from one of the intra-operative procedures is shown in Figure 19.

The patient's skin surface model was then aligned to the meshes so that the pointer-tip and the end of the pointer shaft could be marked relative to the skin surface. These models and markings were exported from *MeshLab* as stereolithography (STL) files. These STL files could then be imported



Figure 19. Aligned 3D point clouds in *MeshLab* following a ‘Point Based Glueing’ and ICP registration process. The patient’s face and identifying features, though relevant for the registration process, are blurred in the image.

into *3D Slicer*, where the points indicating the pointer-tip and end of the pointer shaft were stored as Markups Fiducials for computation, and converted to models using the *Markups To Model* extension to visualize the points as shown in Figure 20.

3.6 Definition and Computation of Performance Metrics

With the denoted drill location and drill angle defined from the pointer-tip and the end of the pointer shaft stored as Markups Fiducials in *3D Slicer*, performance metrics could be computed from each trainee and attending neurosurgeon as compared to the drill location and drill angle defined by the clinical gold-standard. To compute the metrics described in this section, a custom *3D Slicer* module was developed which gives the user the ability to select the desired sets of Markups Fiducials to compare, and computes all desired metrics based on their selection.

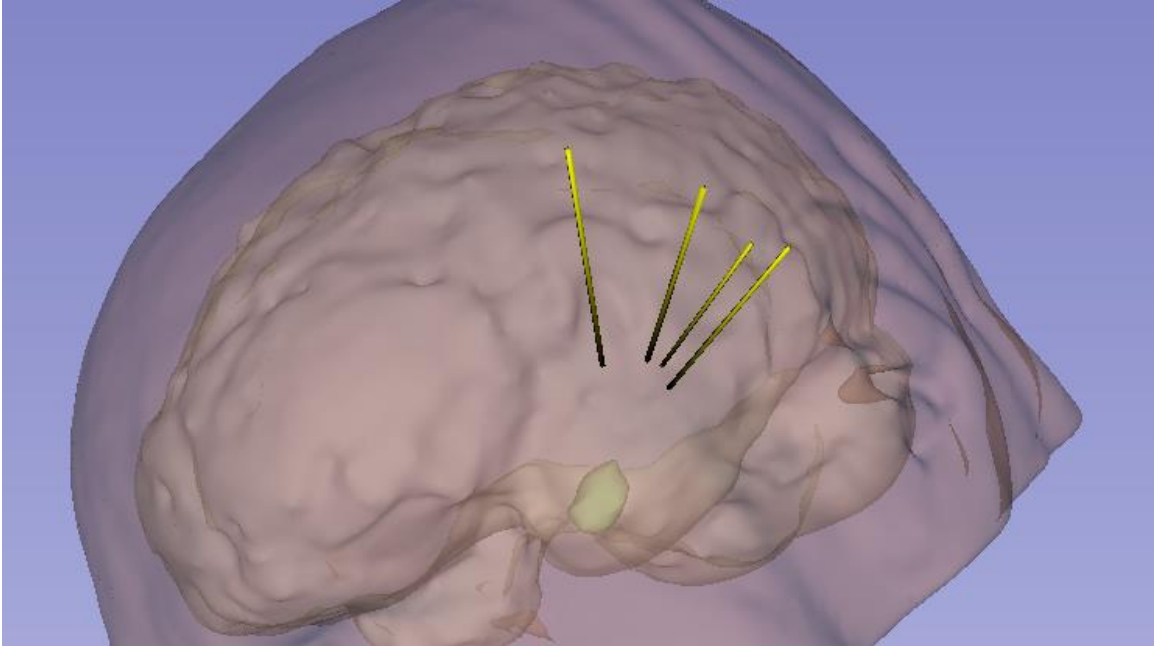


Figure 20. Pointer trajectories, shown in yellow, obtained from aligned 3D point clouds shown on models of the patient’s intra-cortical lesion, brain and skin surface in *3D Slicer*.

The defined metrics were computed based on the geometric properties of the trajectory from each trainee and attending neurosurgeon, and not based on their clinical feasibility or likelihood for surgical success. This was done as it was desired to compare how the trainees performed and selected trajectories compared to the optimal choice that was produced by the attending neurosurgeon at the time of the procedure.

The comparison was based on four metrics, where two of the metrics measured distances and two measured angles. For each of the four defined metrics, an explanation of the metric, the rationale for use, and the equation for computation are described in detail below. A visual representation of the metrics is given in Figure 21.

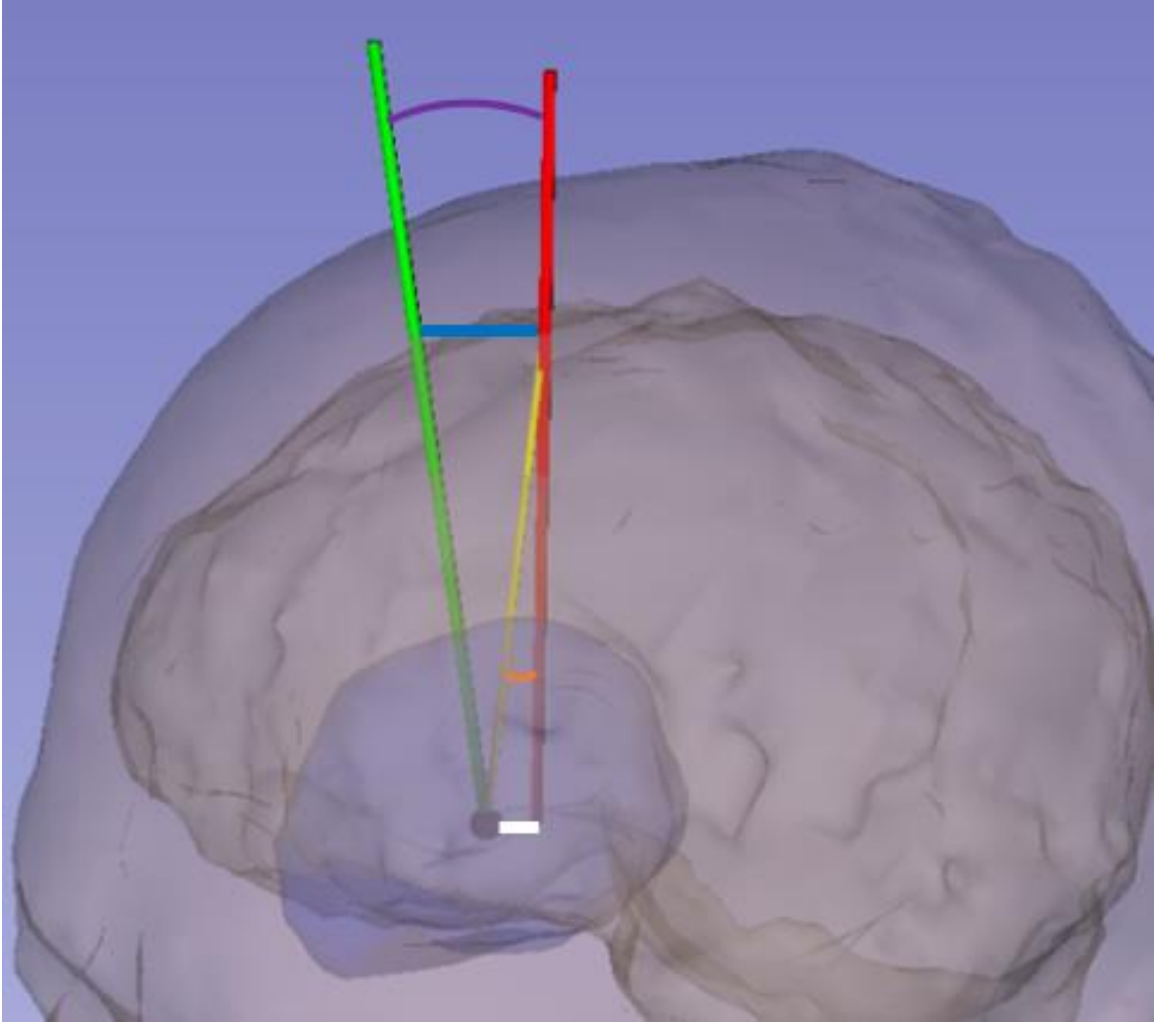


Figure 21. 3D models of surface anatomy, brain, intra-cortical lesion, and user-defined trajectories from one localization task in the simulated study. The black point shows the lesion's geometric center; the green line shows the clinical gold-standard drill location and drill angle; the red line shows the participant's drill location and drill angle; the yellow line shows the trajectory from the participant's drill location to lesion's center; the blue line shows the drill-tip distance; the white line shows the distance to lesion; the purple arc shows the drill angle error; the orange arc shows the angle to lesion.

3.6.1 Drill-tip Distance

The distance between participant drill-tip location and clinical gold-standard drill-tip location (drill-tip distance) was measured. This represented the distance that the participant was from the clinical

gold-standard. Drill-tip distance was computed as the Euclidean distance between i) the participant's pointer-tip location and ii) the clinical gold-standard drill-tip location.

Where the point A represents the location of the pointer-tip, and the point B represents the location of the clinical gold-standard drill-tip, drill-tip distance is:

$$\text{Drill-tip distance} = \sqrt{(A_x - B_x)^2 + (A_y - B_y)^2 + (A_z - B_z)^2}$$

3.6.2 Distance to Lesion

The distance between participant drill trajectory and the lesion's center as defined by the clinical gold-standard (distance to lesion) was measured. This represented the distance that the participant's trajectory was from intersecting the center of the lesion. Distance to lesion was computed as the closest distance between a line and a point. The line used was defined by the participant's pointer-tip location and the end of the pointer shaft and the point used was that defined in the center of the lesion by the clinical gold-standard.

Where the point A represents the location of the pointer-tip, the point B represents the location of the end of the pointer shaft, and the point C represents the location of the center of the lesion as defined by the clinical gold-standard, distance to lesion is:

$$\text{Distance to lesion} = \frac{|(B - A) \times (A - C)|}{|B - A|}$$

3.6.3 Drill Angle Error

The angle between the participant drill trajectory and clinical gold-standard drill trajectory (drill angle error) was measured. This represented the angular error in the participant's trajectory relative to the clinical gold-standard. Drill angle error was computed as the angle between the vectors i) defined by the participant's pointer-tip location and the end of the pointer shaft and ii) defined by the clinical gold-standard drill-tip location and the center of the lesion given by the clinical gold-standard.

Where the vector A is formed by the participant's pointer-tip location and the end of the pointer shaft, the vector B is formed by the clinical gold-standard drill-tip location and the center of the lesion as defined by the clinical gold-standard, drill angle error is:

$$\text{Drill angle error} = \cos^{-1} \left(\frac{\vec{A} \cdot \vec{B}}{\|\vec{A}\| \|\vec{B}\|} \right)$$

3.6.4 Angle to Lesion

The angle between the participant drill trajectory and trajectory between the participant access point and the lesion's center (angle to lesion) was measured. This represented the angular error if the participant's pointer-tip was assumed to be optimal, in the participant's trajectory relative to the center of the lesion given by the clinical gold-standard. Angle to lesion was computed as the angle between the vectors i) defined by the participant's pointer-tip location and the end of the pointer shaft and ii) defined by the participant's pointer-tip location and the center of the lesion given by the clinical gold-standard.

Where the vector A is formed by the participant's pointer-tip location and the end of the pointer shaft, the vector B is formed by the participant's pointer-tip location and the center of the lesion as defined by the clinical gold-standard, angle to lesion is:

$$\text{Angle to lesion} = \cos^{-1} \left(\frac{\vec{A} \cdot \vec{B}}{\|\vec{A}\| \|\vec{B}\|} \right)$$

Completion time was not measured in this study. Though efficiency will be relevant for a fully-fledged training curriculum, it was not relevant for determining if AR was suitable for creating a teaching platform and for determining if the overall performance metrics could be differentiated between trainees and attending neurosurgeons.

3.7 Statistical Analysis

The ability to measure and use participant performance metrics to distinguish between levels of competency were the primary outcome measures of this study. This was done by comparing the performance metrics of trainees and attending neurosurgeons and by determining whether the use of AR technology better informs the wearer where to place their surgical drill and at what angle to drill in to achieve the optimal surgical trajectory. Drill locations and drill angles identified by trainees and attending neurosurgeons were directly compared by observing performance using the 2D and AR methods as compared to the defined clinical gold-standard for the three aforementioned types of neurosurgical procedures. The position of the craniotomy or burr hole and the trajectory to the lesion using this standard of care technique were considered controls.

The performance results of trainees and attending neurosurgeons were compared between each of the 2D and AR methods to determine if the use of AR was beneficial to their performance. The performance results of the 2D and AR methods were compared between trainees and attending neurosurgeons to determine if the developed metrics were capable of distinguishing different levels of competency.

3.8 Results and Discussion

Differences between metrics computed from the 2D and AR methods for trainees and attending neurosurgeons were tested using a two-tailed Mann-Whitney U test. Results for each metric are presented as mean [minimum–maximum]. *P*-values only given for significant results. Trainee (n = 15) and attending neurosurgeon (n = 15) performance in the study is summarized in Table 3.

Differences between trainees and attending neurosurgeon performance when using the 2D and AR methods were tested using a two-tailed Mann-Whitney U test. Results for each metric are presented as mean [minimum–maximum]. *P*-values only given for significant results. Trainee (n = 15) and attending neurosurgeon (n = 15) performance for each planning method is summarized in

Table 4.

Table 3. 2D and AR method performance comparison.

	Metric	2D Method	AR Method	<i>p</i>
Trainee	Drill-tip distance [mm]	33 [13–68]	21 [2–44]	
	Distance to lesion [mm]	19 [5–49]	13 [1–43]	
	Drill angle error [°]	37 [9–84]	29 [11–57]	
	Angle to lesion [°] *	29 [4–67]	17 [1–53]	0.03
Attending Neurosurgeon	Drill-tip distance [mm]	13 [5–28]	10 [4–21]	
	Distance to lesion [mm]	11 [4–20]	10 [3–20]	
	Drill angle error [°]	18 [3–28]	18 [2–35]	
	Angle to lesion [°]	13 [5–27]	13 [3–36]	

* Indicates significance between 2D and AR metrics in a participant group.

Table 4. Trainee and attending neurosurgeon performance comparison.

	Metric	Trainee	Attending Neurosurgeon	<i>p</i>
2D Method	Drill-tip distance [mm] *	33 [13–68]	13 [5–28]	0.001
	Distance to lesion [mm]	19 [5–49]	11 [4–20]	
	Drill angle error [°]	37 [9–84]	18 [3–28]	
	Angle to lesion [°] *	29 [4–67]	13 [5–27]	0.009
AR Method	Drill-tip distance [mm] *	21 [2–44]	10 [4–21]	0.011
	Distance to lesion [mm]	13 [1–43]	10 [3–20]	
	Drill angle error [°] *	29 [11–57]	18 [2–35]	0.032
	Angle to lesion [°]	17 [1–53]	13 [3–36]	

* Indicates significance between trainee and attending neurosurgeon metrics for a given planning method.

The intra-operative study provides a proof of concept that the *HoloLens* and *HoloQuickNav* may have the potential to be used for identifying optimal drill locations and drill angles in neurosurgical procedures. While changes in performance were observed in the trainee group, only one of four of these differences were statistically significant. There were measurable changes between the neurosurgeon group as well, however, these changes were smaller in magnitude and not statistically significant. As such, while the *HoloLens* may provide neurosurgeons with enhanced visualizations

of patient anatomy and potentially reduce the level of difficulty for a given procedure, our results show that it does not significantly affect their ability to form a surgical plan when compared to conventional methods. Changes in performance are observed between trainees and attending neurosurgeons when using a given planning method, with two of four differences in metrics being statistically significant for both the 2D and AR methods.

CBME compliant metrics must be relevant, valid, objective, and transparent. From our study, it is clear that our metrics are relevant. Creating a burr hole in any of our target procedures is a key task wherein the learning objectives involve selecting the proper location of the drill site on the skull, and the key performance metrics require a burr hole placed in the acceptable region and an appropriate perforation angle at the surface [76]. The proposed metrics are valid, as they can differentiate between trainees and attending neurosurgeon skill levels, as seen in

Table 4, and shown most clearly through the Drill-tip distance, Drill angle error, and Angle to lesion metrics. The proposed metrics are objective, as they are computed directly from the geometric properties of the user's drill location and drill angle localization with respect to the optimal. Additionally, the metrics are transparent, as they are simple to interpret geometrically and the concept surrounding the choice of metric is clear. However, our defined metrics can not measure surgical outcomes and have no defined threshold for determining success. Though they appear clinically relevant, it is not clear if the improvements in performance observed while using the *HoloLens* have any effect on the success of the procedure or to patient outcome.

Through the period in which the study was conducted, 19 cases met the study's inclusion criteria and were available for patient enrolment. Fifteen cases were attended, in the remaining four cases; one patient did not consent to participate, one case could not be completed due to technical problems with the *HoloLens*, and two cases could not be completed due to the absence of required research personnel. As such, cases were not selected based on perceived difficulty or potential results. However, it is clear that additional cases are required to determine whether experts can

benefit from this technology by adapting it to their routine, or if it is primarily of benefit to less experienced operators in achieving better accuracy at an early phase of their learning curve.

3.9 Summary

This chapter has presented the design and methodology for an intra-operative assessment of trainee and attending neurosurgeon performance, and a validation of the developed metrics. This work has validated a study protocol, intra-operative workflow, data collection and processing pipeline for using and evaluating AR technology in a clinical environment.

With the performance of trainees and attending neurosurgeons having been successfully assessed, it has become clear that the defined metrics are relevant, valid, objective, and transparent. These metrics are also capable of differentiating between different levels of expertise, a key factor that is required for CBME compliance.

Chapter 4

Simulated Target Localization

4.1 Study Design

To assess the effectiveness of *HoloQuickNav* for optimal drill location and drill angle identification in a medical education setting, a simulated-based phantom study was conducted to assess the performance of the software compared to other conventional medical image visualization methods. Seven medical student trainees were recruited from the Queen's University School of Medicine to localize drill locations and drill angles on a phantom using three different visualization methods. All medical students had little or no prior simulated or clinical surgical experience.

The three visualization methods consisted of a computer display with 2D CT or MRI images (2D method) (Figure 22a), a computer display with 2D CT or MRI images and a 3D visualization of the phantom's skin surface, brain, and intra-cortical lesion (3D method) (Figure 22b), and a 3D holographic visualization of the phantom's skin surface, brain, and intra-cortical lesion shown on a *HoloLens* running *HoloQuickNav* (AR method) (Figure 22c). Each visualization displayed an annotated surgical path, defined by an attending neurosurgeon, to be localized by the participants during the study. In the 2D images, the annotated surgical path was indicated by a red line shown on the images. In the 3D view and holographic visualizations, the surgical path was indicated by a model of a red cylinder.

4.2 Experimental Setup

An optical tool tracking setup was implemented using a series of four *OptiTrack Prime 17W* cameras (NaturalPoint Inc., Corvallis, Oregon, USA) to record the drill locations and drill angles during each trial. A series of optical tracking markers were affixed to the phantom and pointer tool to capture participant localizations. The *PLUS Server Application* software interface for hardware components [16] was used to acquire and send tracking data to *3D Slicer* via the *OpenIGTLink*

network protocol [15]. Within *3D Slicer*, all pose information was recorded using the Sequence Browser module within the *Sequences* extension [14].

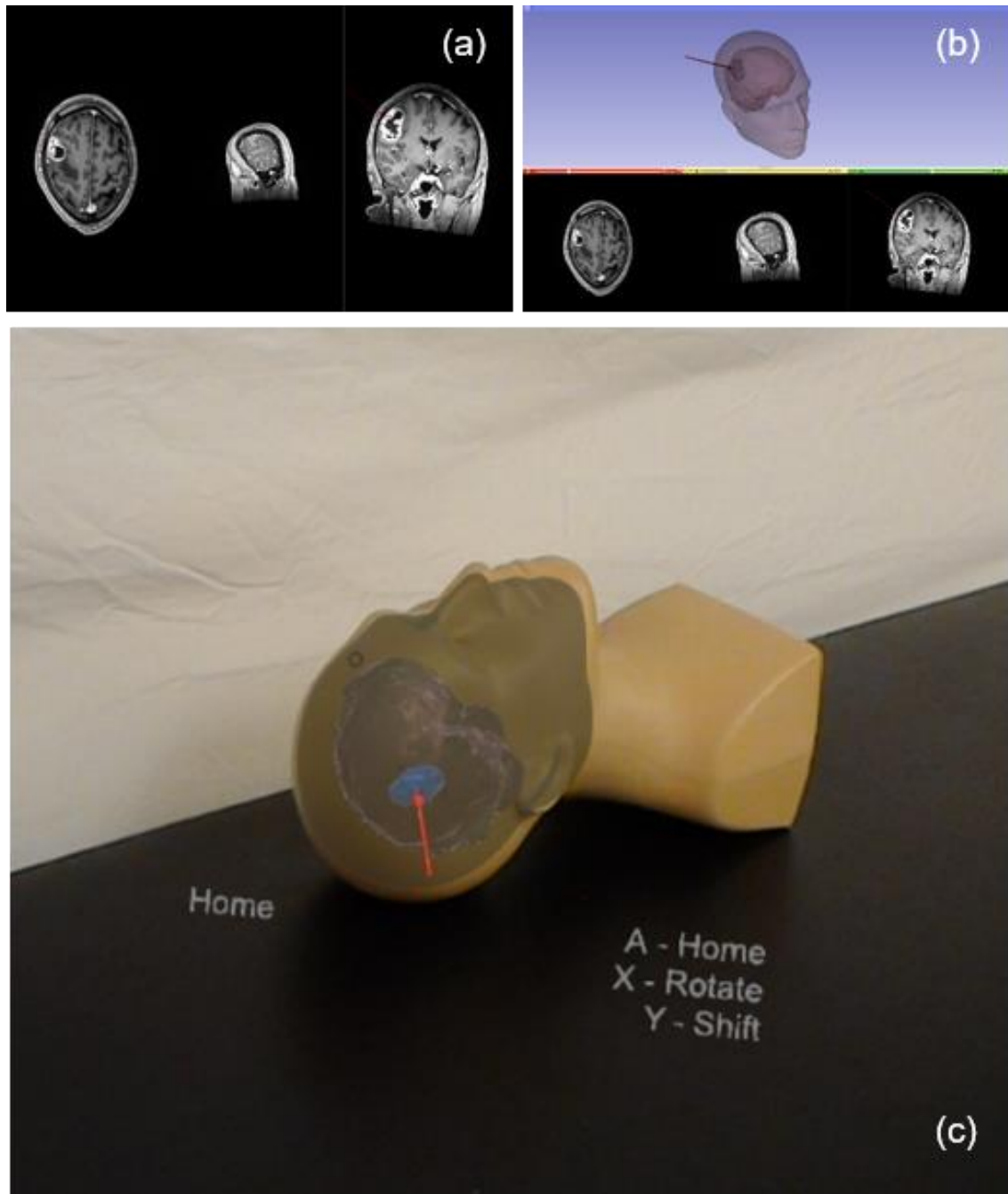


Figure 22. Views of visualizations provided to the user in the phantom study while using the (a) 2D Method, (b) 3D Method, and (c) AR Method in an image series used in the study.

Participants were assigned a set of 14 image series; each series was used with only one of the three visualization methods, and all trials were completed in a random order. The images and associated models were deformably registered to the phantom used as a phantom for the study. Participants were able to browse through the images and models displayed in the various visualization methods. Additionally, participants were timed and given a target time to complete each target localization of two minutes. They were not stopped if they had not completed the task within two minutes. In each trial, participants localized the drill location and drill angle to the best of their ability based on the information shown on the computer display or on the *HoloLens* using the optically tracked pointer tool.

Denoted drill locations and drill angles were compared to that which was defined by an attending neurosurgeon prior to the study. Following the study, operators answered a subjective multidimensional questionnaire to assess the workload and effectiveness of the 2D, 3D, and AR methods. This questionnaire was based on the NASA Task Load Index, a subjective and multidimensional assessment tool that rates the perceived workload for assessing a task's effectiveness [77].

4.3 Data Processing

To process the acquired pose information that was collected during all sessions of the simulated target localization study, the points indicating the target drill location and drill angle and the participant's pointer-tip and end of the pointer shaft were stored as Markups Fiducials for computation, similarly to the procedure in Section 3.5 (Data Processing). Each of the target drill locations and drill angles, defined by an attending neurosurgeon (Figure 23a), were annotated to mark a point at the center of the target, and at the surgical access point – where the drill-tip would be placed (Figure 23b). Next, each participant denoted drill location and drill angle (Figure 23c) was converted to two points; the pointer-tip and the end of the pointer shaft (Figure 23d).

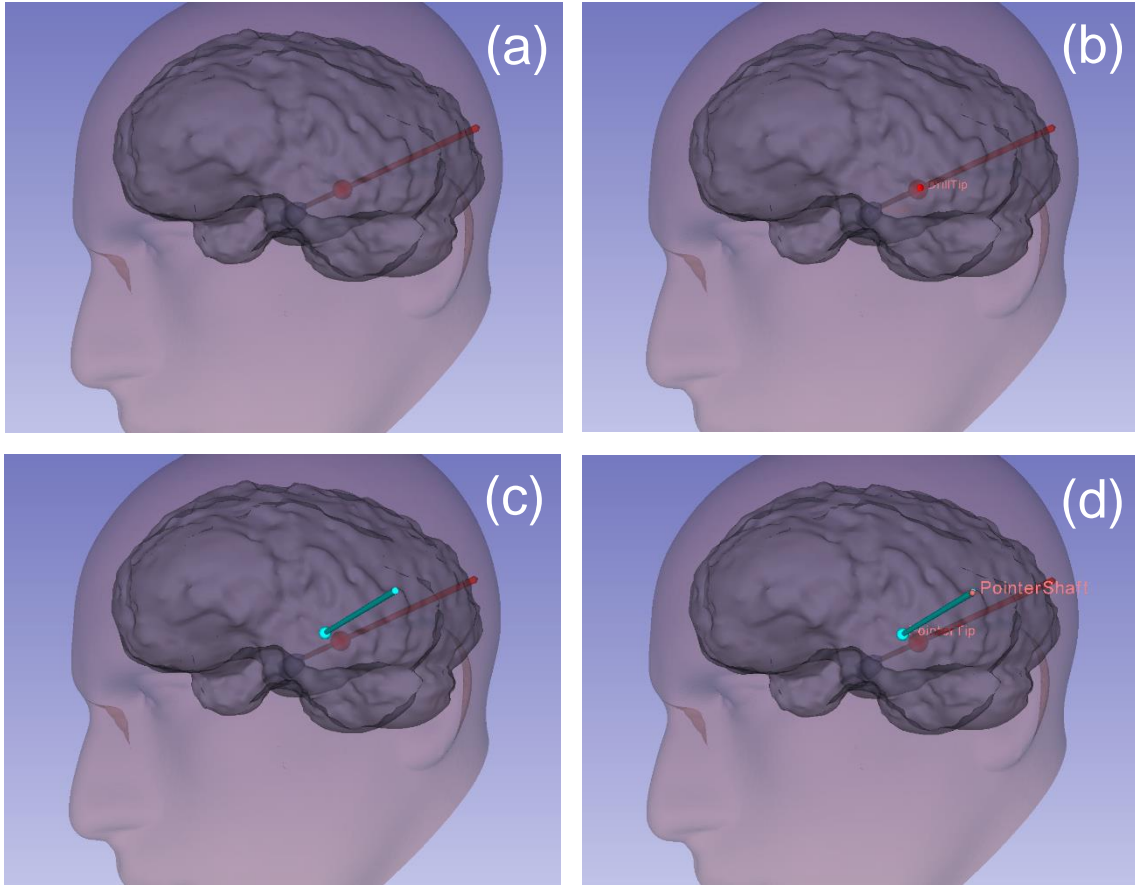


Figure 23. Views in *3D Slicer* of the phantom head and deformably registered brain and intra-cortical lesion models for one trial of the simulated study showing (a) the target drill location and drill angle (red line) as defined by an attending neurosurgeon, (b) the Markups Fiducials annotating the target within the intra-cortical lesion and the drill location, (c) the participant’s pointer (blue line) denoted drill location and drill angle relative to the target drill location and drill angle, and (d) the Markups Fiducials annotating the pointer-tip and the end of the pointer shaft.

4.4 Definition and Computation of Performance Metrics

In this study, the comparisons were based on the same metrics described in Section 3.6 (Definition and Computation of Performance Metrics), with the exception that the clinical gold-standard in each case was not defined in the operating room at the time of the study, but had been previously denoted by an attending neurosurgeon on the phantom prior to the study. Metrics were computed using the same custom *3D Slicer* module that was previously developed and discussed.

Additionally, the completion time was recorded for each localization to provide a sense of time pressure between the different visualization tasks for participants.

4.5 Results and Discussion

A summary of the participant ($n = 7$) metrics from their localizations ($n = 14$ per participant) using the 2D, 3D and AR methods are presented in Table 5. Results are presented as mean [minimum–maximum].

Table 5. 2D, 3D, and AR method performance summary.

Metric	2D Method	3D Method	AR Method
Drill-tip distance [mm]	65 [8–156]	26 [3–171]	12 [2–26]
Distance to lesion [mm]	29 [5–80]	18 [1–58]	12 [1–23]
Drill angle error [°]	63 [2–173]	24 [1–151]	8 [1–19]
Angle to lesion [°]	30 [8–75]	31 [1–106]	17 [2–55]
Completion time [s]	126 [41–225]	75 [17–171]	42 [15–126]

Differences between the computed metrics from each of the different visualization methods were tested using the Mann-Whitney U test, using Bonferroni correction for multiple tests ($\alpha = 0.01$). Resulting p -values from each statistical test are presented in Table 6.

Table 6. Pairwise performance comparison of 2D, 3D, and AR method target localization metrics.

Metric	2D v. 3D	2D v. AR	3D v. AR
Drill-tip distance	0.003*	< 0.001*	0.008*
Distance to lesion	0.007*	< 0.001*	0.047
Drill angle error	0.004*	< 0.001*	< 0.001*
Angle to lesion	0.57	< 0.001*	0.034
Completion time	< 0.001*	< 0.001*	< 0.001*

* Indicates significance at the Bonferroni corrected alpha value.

Participants localized a drill location and drill angle. Participants localized these on the correct side of the phantom’s head in 67% of tasks using the 2D method, 97% of tasks using the 3D method,

and 100% of tasks using the AR method. Furthermore, participants localized the drill location and drill angle within the target time of two minutes in 55% of tasks using the 2D method, 88% of tasks using the 3D method, and 97% of tasks using the AR method. These values are particularly encouraging when looking not only at the skill of drill location and drill angle localization but at one which is even more fundamental; that of correctly interpreting the orientation of a series of CT or MRI images. As only 67% of the trials completed using the 2D Method saw the participant localize a trajectory on the correct side of the phantom, it stands that several of the medical students who were recruited as participants lack this fundamental skill. However, when given access to the imaging alongside 3D or AR visualizations, this increased to 97% and 100% respectively.

The simulated study demonstrated significant improvements in performance when users completed their drill location and drill angle localizations using the 3D and AR methods when compared to traditional 2D methods. This result is consistent with the literature wherein 3D and AR visualizations better facilitate and provide benefits to a user's perception of spatial relations between images or models on a screen and real-world objects, such as patients or phantoms [39]. Additionally, the study demonstrated significant improvements over the 3D method when using the AR method, most saliently with a reduction in the mean completion time of over 40% between the two methods. This illustrates the potential impact of augmented environments and AR technology for increasing the efficiency of surgical planning intra-operatively.

The variability in space of the holographic models produced by the *HoloLens* as the user moves has been estimated to be approximately 5 mm [78]. The error attributed to the registration process was 5–10 mm over 50% of the time, when performed by novices. It is of note that the mean distance to the preplanned drill location for trainees in a simulated training environment (12 mm) and clinical setting (21 mm) were higher than these values, even when the variability and registration error are combined. This reveals that participants were not able to mitigate the holographic instability. While it is valuable to see that some trainees were able to localize the access points

within the range of the variability and registration error, at present this error is still too high for clinical use. The holographic variability, registration processes, and training that accompany this technology must be improved before use for decision making on patients can begin. However, given the *HoloLens*'s ability to provide direct 2D and 3D visualizations in the operative field, this type of technology may prove beneficial for simulation and training of medical students and surgical residents in simulated and clinical settings. As such, the *HoloLens* and related AR HMD technologies may hold potential for training and simulation-based education or planning of various neurosurgical procedures [63, 75, 79].

A summary of responses to the post-study questionnaire is given in Figure 24. Responses showed that, on average, users felt the AR method was less mentally demanding, less hurried or rushed, more successful, and required users to work less hard than the 2D and 3D methods. The AR method was comparable to the 3D method in terms of how discouraged, irritated, stressed or annoyed it made the users. It was comparable to the 2D and 3D methods in terms of how physically demanding the task was. These results illustrate that in addition to quantitatively allowing participants to perform better, they also underwent less mental work and were under less time pressure while performing at overall higher levels of performance. The positive results from the questionnaire highlight the potential for this technology to be used in surgical applications or simulation-based approaches for teaching skills and building confidence in trainees.

Lastly, a limitation of both the simulated and clinical studies involved the recruitment of all participants from the same institution. Trainees were recruited from the Queen's University School of Medicine and Queen's University General Surgery residency program and most had little or no prior experience with HMD AR technology or with surgical planning. Furthermore, many trainees in the simulation study had little to no experience in reading and interpreting medical images. To further demonstrate these results, future studies would be required at multiple institutions with

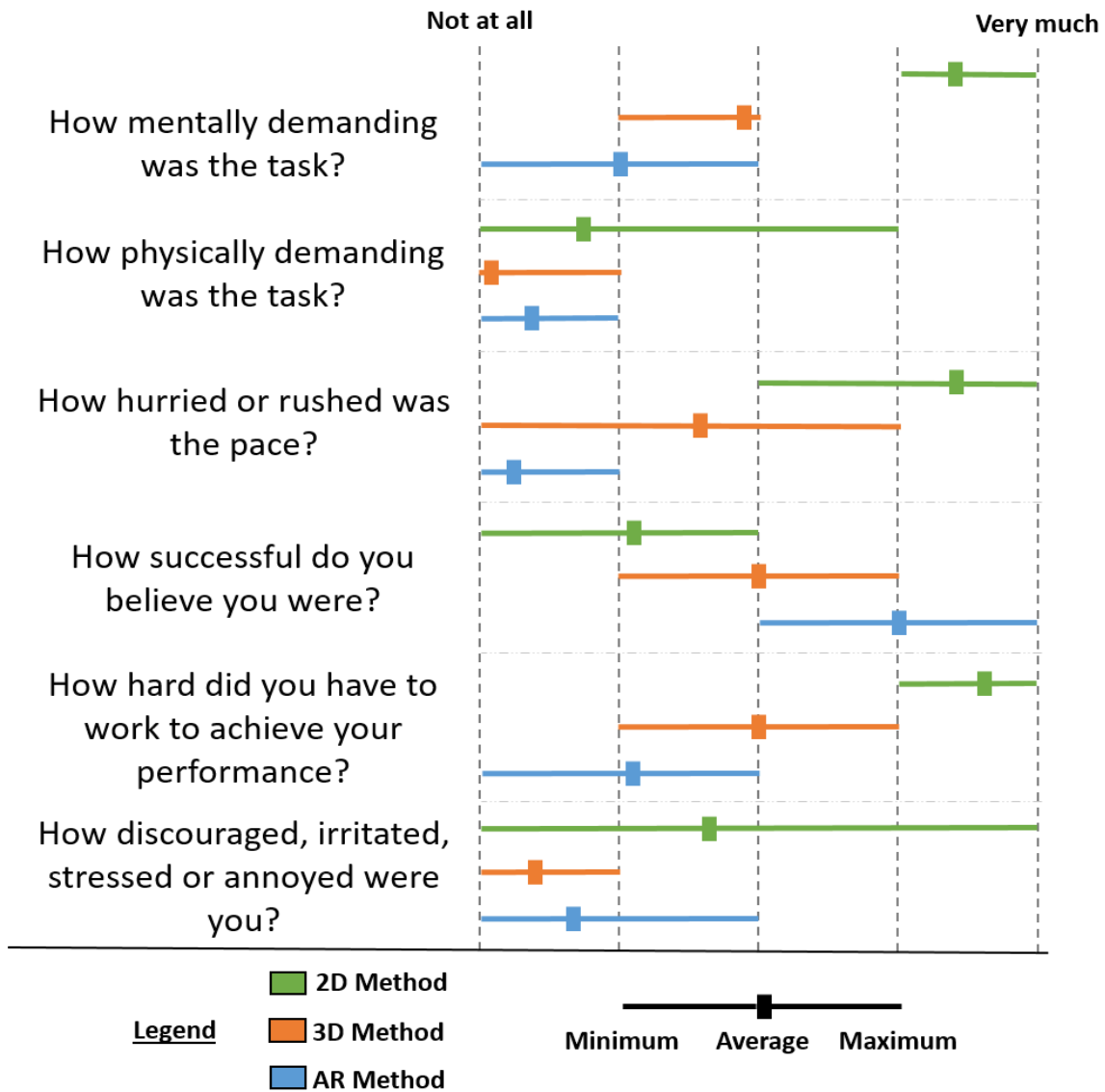


Figure 24. Min-max-average assessment of post-study questionnaire responses.

participants of all skill levels. In both this study, and in the clinical feasibility study, the sample size is a further limitation to illustrating statistical power.

4.6 Summary

This chapter has presented the design and methodology for a simulation-based education study, wherein the performance of trainees in localizing drill locations and drill angles with AR and two other conventional visualization methods was assessed. This work validated the utility of AR in

reducing the difficulty of the target localization task while aiding participants in increasing their performance.

With the performance and utility of AR having been assessed compared to two other conventional visualization methods, it is clear that AR was able to provide sufficient decision making support to improve trainee performance. Additionally, AR facilitated the process of localizing targets on simulated patients in a manner which was less demanding and less difficult for participants.

Chapter 5

Future Work and Conclusions

5.1 Future Work

The proposed system shows promise for use in a neurosurgical training curriculum. This technology can be used as a training platform which would allow trainees to have their improvements monitored relative to established performance benchmarks, using the established and demonstrated metrics that have been presented, as they progress through a curriculum to aid them in planning and targeting neurosurgical procedures. This system, and training with it, stands to have the greatest impact in the first and second stages of CBME-based residency programs as trainees begin a transition into their position, and gain foundational skills. The first stage, ‘transition to discipline’, focuses on the orientation and assessment methods of a trainee. The second stage, ‘foundations of discipline’, ensures that the broader competencies required for success in the field are covered before the trainee may progress to the final stages, ‘core of discipline’ and ‘transition to practice’. In the first two stages, promoting a method for objective performance assessment in a foundational skill, such as determining and localizing a drill location and drill angle, may be of critical importance to a trainee’s progression and learning.

For practical curriculum development, there are two changes this platform would require. First, metrics must be computed from a clinical gold-standard that is derived from a consensus of expert attending neurosurgeons. This will ensure that instead of needing to match exactly with the optimal trajectory defined by one attending neurosurgeon, at the time of the procedure, trainees will seek to ensure their trajectories fall into a 3D cone of consensus. This cone could be defined to ensure that all expert trajectories are encapsulated, or it could be defined as the mean of all expert trajectories with a tolerance of one standard deviation. In this sense, the essence of the metric is unchanged, but the computation and tolerance for establishing competence are modified. Secondly,

determining the number and frequency of simulated training sessions required on the path to competency will be critical to ensuring the developed curriculum gives trainees the ability to practice until they become entrustable.

This technology may allow methods for providing objective and measurable feedback as these metrics are geometric in nature. This ensures that trainees can practice the development of this skillset autonomously without expert supervision – an important component of the competency-based medical education paradigm that is rapidly evolving at medical schools around the world. By ensuring that trainees select a trajectory within the cone of consensus, it could be confirmed the trainee has selected an appropriate trajectory. Given the metrics that were established for drill location and drill angle localization are not neurosurgery-specific and the setup is readily replicable, it is foreseeable that this system could be used for the analysis of planning and targeting effectiveness in other surgical specialties.

As the *HoloQuickNav* platform is now available – and has been validated for simulated training and intra-operative use – I propose that in future work, a curriculum consisting of a series of simulation-based training sessions be developed. The AR platform must be compared against existing learning tools and visualization methods for achieving competence in neurosurgical planning. It must be assessed whether this technology allows trainees to reach competency sooner or with reduced cognitive effort than with other methods.

5.2 Conclusions

The results obtained in this work indicate that our HMD AR technology can measurably improve surgical planning and target localization in clinical and simulated training settings for trainees. The feasibility and usefulness of the *HoloLens* were validated for identifying optimal drill location and drill angle in a clinical environment, and this work has led to the development of metrics which allow for significant differentiation between levels of competence in multiple areas. Furthermore,

trainees rate this technology equally or more helpful compared to conventional visualization methods.

Bibliography

- [1] T. Peters and K. Cleary, *Image-guided interventions: technology and applications*, Springer, 2008.
- [2] D. Brenner, C. Elliston, E. Hall and W. Berdon, "Estimated risks of radiation-induced fatal cancer from pediatric ct," *American Journal of Roentgenology*, vol. 176, no. 2, pp. 289-296, 2001.
- [3] F. Pohlig, C. Kirchhoff, U. Lenze, J. Schauwecker, R. Burgkart, H. Rechl and R. von Eisenhart-Rothe, "Percutaneous core needle biopsy versus open biopsy in diagnostics of bone and soft tissue sarcoma: a retrospective study," *European Journal of Medical Research*, vol. 17, no. 1, p. 29, 2012.
- [4] M. B. El-Tamer, B. M. Ward, T. Schiffner, L. Neumayer, S. Khuri and W. Henderson, "Morbidity and mortality following breast cancer surgery in women: national benchmarks for standards of care," *Annals of Surgery*, vol. 245, no. 5, p. 665, 2007.
- [5] V. J. Zannis and K. M. Aliano, "The evolving practice pattern of the breast surgeon with disappearance of open biopsy for non-palpable lesions," *The American Journal of Surgery*, vol. 176, no. 6, pp. 525-528, 1998.
- [6] P. Ferroli, G. Tringali, F. Acerbi, M. Schiariti, M. Broggi and D. B. G. Aquino, "Advanced 3-dimensional planning in neurosurgery," *Neurosurgery Supplemental*, vol. 1, no. 1, pp. A54-A62, 2013.
- [7] T. Y. Jung, S. Jung, Y. Kim, S. J. Park, S. S. Kang, S. Kim and S. C. Lim, "Application of neuronavigation system to brain tumour surgery with clinical experience of 420 cases," *Minimally Invasive Neurosurgery*, vol. 49, no. 4, pp. 210-215, 2006.
- [8] J. Wadley, N. Dorward, N. Kitchen and D. Thomas, "Pre-operative planning and intra-operative guidance in modern neurosurgery: a review of 300 cases," *Annals of the Royal College of Surgeons of England*, vol. 81, no. 4, pp. 217-225, 1999.
- [9] T. Koivukangas, J. P. Katisko and J. P. Koivukangas, "Technical accuracy of optical and the electromagnetic tracking systems," *SpringerPlus*, vol. 2, no. 1, pp. 1-7, 2013.
- [10] U. Mezger, C. Jendrewski and M. Bartels, "Navigation in surgery," *Langenbecks Archives of Surgery*, vol. 398, pp. 501-514, 2013.

- [11] W. Birkfellner, F. Watzinger, F. Wanschitz, R. Ewers and H. Bergmann, "Calibration of tracking systems in a surgical environment," *IEEE Transactions on Medical Imaging*, vol. 17, no. 5, pp. 737-742, 1998.
- [12] F. Kral, E. J. Puschban, H. Riechelman and W. Freysinger, "Comparison of optical and electromagnetic tracking for navigated lateral skull base surgery," *The International Journal of Medical Robotics and Computer Assisted Surgery*, vol. 9, no. 2, pp. 247-252, 2013.
- [13] T. Ungi, A. Lasso and G. Fichtinger, "Open-source platforms for navigated image-guided interventions," *Medical Image Analysis*, vol. 33, pp. 181-186, 2016.
- [14] A. Fedorov, R. Beichel, J. Kalpathy-Cramer, J. Finet, J. C. Fillion-Robin, S. Pujol, C. Bauer, D. Jennings, F. Fennessy, M. Sonka, J. Buatti, S. Aylward, J. V. Miller, S. Pieper and R. Kikinis, "3D Slicer as an image computing platform for the quantitative imaging network," *Magnetic Resonance Imaging*, vol. 30, pp. 1323-1341, 2012.
- [15] J. Tokuda, G. S. Fisher, X. Papademetris, Z. Yaniv, L. Ibanez, P. Cheng, H. Liu, J. Blevins, J. Arata, A. J. Golby, T. Kapur, S. Pieper, E. C. Burdette, G. Fichtinger, C. M. Tempany and N. Hata, "OpenIGTLink: an open network protocol for image-guided therapy environment," *International Journal of Medical Robotics and Computer Assisted Surgery*, vol. 5, no. 4, pp. 423-434, 2009.
- [16] A. Lasso, T. Heffter, A. Rankin, C. Pinter, T. Ungi and G. Fichtinger, "PLUS: open-source toolkit for ultrasound-guided intervention systems," *IEEE Transactions on Biomedical Engineering*, vol. 61, no. 10, pp. 2527-2537, 2014.
- [17] M. Kersten-Oertel, I. J. Gerard, S. Drouin, K. Petrecca, J. A. Hall and D. L. Collins, "Towards augmented reality guided craniotomy planning in tumour resections," in *7th International Conference on Medical Imaging and Augmented Reality*, Bern, 2016.
- [18] M. Blackwell, C. Nikou, M. DiGioia and T. Kanade, "An image overlay system for medical data visualization," in *First International Conference on Medical Image Computing and Computer Assisted Intervention*, Cambridge, 1998.
- [19] F. Sauer, A. Khamene and S. Vogt, "An augmented reality navigation system with a single-camera tracker: system design and needle biopsy phantom trial," in *Medical Image Computing and Computer-Assisted Intervention*, Tokyo, 2002.
- [20] H. Hua, C. Gao, J. P. Rolland and F. Biocca, "An ultra-light and compact design and implementation of head-mounted projective displays," in *IEEE Virtual Reality Conference*, Yokohama, 2001.

- [21] W. Birkfellner, M. Figl, K. Huber, F. Watzinger, F. Wanschitz, J. Hummel, R. Hanel, W. Greimel, P. Homolka and R. Ewers, "A head-mounted operating binocular for augmented reality visualization in medicine-design and initial evaluation," *IEEE Transactions on Medical Imaging*, vol. 21, no. 8, pp. 991-997, 2002.
- [22] J. Wu, M. Wang, K. Liu, M. Hu and P. Lee, "Real-time advanced spinal surgery via visible patient model and augmented reality system," *Computer Methods and Programs in Biomedicine*, vol. 113, pp. 869-881, 2014.
- [23] G. Fichtinger, S. J. Zinreich, A. Deguet, G. Fischer, I. Iordachita, E. Balogh, K. Masamune, R. H. Taylor, L. Fayad and M. de Oliveira, "Image overlay for ct-guided needle insertions," *Computer Aided Surgery*, vol. 10, no. 4, pp. 241-255, 2005.
- [24] G. Fichtinger, A. Deguet, K. Masamune, E. Balogh, G. S. Fisher, H. Mathieu, R. H. Taylor, S. J. Zinreich and L. Fayad, "Image overlay guidance for needle insertion in ct scanner," *IEEE Transactions on Biomedical Engineering*, vol. 52, no. 8, pp. 1415-1424, 2005.
- [25] S. Vikal, P. U-Thainual, J. A. Carrino, I. Iordachita, G. S. Fisher and G. Fichtinger, "Perk station-percutaneous surgery training and performance measurement platform," *Computerized Medical Imaging and Graphics*, vol. 34, no. 1, pp. 19-32, 2010.
- [26] T. Ungi, C. T. Yeo, U. Paweena, R. C. McGraw and G. Fichtinger, "Augmented reality needle guidance improves facet joint injection training," in *SPIE Medical Imaging*, Orlando, 2011.
- [27] C. T. Yeo, T. Ungi, A. Lasso, R. C. McGraw and G. Fichtinger, "The effect of augmented reality training on percutaneous needle placement in spinal facet joint injections," *IEEE Transactions on Biomedical Engineering*, vol. 58, no. 7, pp. 2031-2037, 2011.
- [28] J. Fritz, P. U-Thainual, T. Ungi, A. J. Flammang, G. Fichtinger, I. Iordachita and J. Carrino, "Augmented reality visualization with use of image overlay technology for mr imaging-guided interventions: assessment of performance in cadaveric shoulder and hip arthrography at 1.5t," *Radiology*, vol. 265, no. 1, pp. 254-259, 2012.
- [29] J. Fritz, P. U-Thainual, T. Ungi, A. J. Flammang, G. Fichtinger, I. Iordachita and J. Carrino, "Augmented reality visualization using image overlay for mr-guided interventions: accuracy for lumbar spinal procedures with a 1.5 tesla mri scanner," *American Journal of Roentgenology*, vol. 198, no. 1, pp. 266-273, 2012.
- [30] J. Fritz, P. U-Thainual, T. Ungi, A. J. Flammang, G. Fichtinger, I. Iordachita and J. Carrino, "Augmented reality visualization using an image overlay system for mr-guided interventions:

- technical performance of spine injection procedures in human cadavers at 1.5 tesla," *European Radiology*, vol. 23, no. 1, pp. 235-245, 2013.
- [31] M. Anand, F. King, T. Ungi, A. Lasso, J. Rudan, J. Jayender, J. Fritz, F. Carrino, A. Jolesz and G. Fichtinger, "Design and development of a mobile image overlay system for image guided needle interventions," in *36th Annual International Conference of IEEE EMBS*, Chicago, 2014.
- [32] Z. M. C. Baum, A. Lasso, T. Ungi and G. Fichtinger, "Real-time self-calibration of a tracked augmented reality display," in *SPIE Medical Imaging*, San Diego, 2016.
- [33] Z. M. C. Baum, T. Ungi, A. Lasso and G. Fichtinger, "Usability of a real-time tracked augmented reality display in musculoskeletal injections," in *SPIE Medical Imaging*, Orlando, 2017.
- [34] C. R. Maurer Jr., F. Sauer, B. Hu, B. Bascle, B. Geiger, F. Wenzel, F. Recchi, T. Rohlfing, C. M. Brown, R. S. Bakos, R. J. Maciunas and A. Bani-Hashemi, "Augmented reality visualization of brain structures with stereo and kinetic depth cues: system description and initial evaluation with head phantom," in *SPIE Medical Imaging*, San Diego, 2001.
- [35] E. C. S. Chen, K. Sarkar, J. H. S. Baxter, J. Moore, C. Wedlake and P. T. M., "An augmented reality platform for planning of minimally invasive cardiac surgeries," in *SPIE Medical Imaging*, San Diego, 2012.
- [36] X. Chen, L. Xu, Y. Wang, H. Wang, F. Wang, X. Zeng, Q. Wang and J. Egger, "Development of a surgical navigation system based on augmented reality using an optical see-through head-mounted display," *Journal of Biomedical Informatics*, vol. 55, pp. 124-131, 2015.
- [37] F. Kellner, B. Bolte, G. Bruder, U. Rautenberg, F. Steinicke and R. Koch, "Geometric calibration of head-mounted displays and its effects on distance estimation," *IEEE Transactions of Visualizations and Computer Graphics*, vol. 18, no. 4, pp. 589-596, 2012.
- [38] B. Vigh, S. Muller, O. Ristow, H. Deppe, S. Holdstock, J. den Hollander, N. Navab, T. Steiner and B. Hohlweg-Majert, "The use of a head-mounted display in oral implantology: a feasibility study," *International Journal of Computer-Assisted Radiology and Surgery*, vol. 9, no. 1, pp. 71-78, 2014.
- [39] K. Abhari, J. H. S. Baxter, E. C. S. Chen, A. R. Khan, T. M. Peters and S. de Ribaupierre, "Training for planning tumour resection: augmented reality and human factors," *IEEE Transactions on Biomedical Engineering*, vol. 62, no. 6, pp. 1466-1477, 2015.

- [40] C. Morales, N. V. Navkar, D. Tsagkaris, A. Webb, T. A. Birbilis, I. Seimenis and N. V. Tsekos, "Holographic interface for three-dimensional visualization of MRI on HoloLens: a prototype platform for mri guided neurosurgeries," in *17th International Conference of Bioinformatics and Bioengineering*, Washington, 2017.
- [41] K. Maruyama, E. Watanabe, T. Kin, K. Saito, A. Kumakiri, A. Noguchi, M. Nagane and Y. Shiokawa, "Smart glasses for neurosurgical navigation by augmented reality," *Operative Neurosurgery*, vol. opx279, pp. 1-6, 2018.
- [42] E. Rae, A. Lasso, M. Holden, E. Morin, R. Levy and G. Fichtinger, "Neurosurgical burr hole placement using the Microsoft HoloLens," in *SPIE Medical Imaging*, Houston, 2018.
- [43] T. Peters, "Image-guidance for surgical procedures," *Physics in Medicine and Biology*, vol. 51, pp. R505-R540, 2006.
- [44] L. Qian, A. Barthel, A. Johnson, G. Osgood, P. Kazanzides, N. Navab and F. B. "Comparison of optical see-through head-mounted displays for surgical interventions with object-anchored 2D-display," *International Journal of Computer Assisted Radiology and Sugery*, vol. 12, no. 6, pp. 901-910, 2017.
- [45] S. Moosburner, C. Remde, P. Tang, M. Queisner, N. Haep, J. Pratschke and I. M. Sauer, "Real world usability analysis of two augmented reality headsets in visceral surgery.," *Artificial Organs*, vol. 00, pp. 1-5, 2018.
- [46] O. M. Tepper, H. L. Rudy, A. Lefkowitz, K. A. Weimer, S. M. Marks, C. S. Stern and E. S. Garfein, "Mixed reality with HoloLens: where virtual reality meets augmented reality in the operating room," *Plastic and Reconstructive Surgery*, vol. 140, no. 5, pp. 1066-1070, 2017.
- [47] H. Durrant-Whyte and T. Bailey, "Simultaneous localization and mapping: part I," *IEEE Robotics & Automation Magazine*, vol. 13, no. 2, pp. 99-110, 2006.
- [48] T. Bailey and H. Durrant-Whyte, "Simultaneous localization and mapping (SLAM): part II," *IEEE Robotics & Automation Magazine*, vol. 13, no. 3, pp. 108-117, 2006.
- [49] A. Ducruet, B. Grobteny, B. Zacharia, Z. Hickman, P. DeRosa, K. Andersen, E. Sussman, A. Carpenter and E. Connolly, "The surgical management of chronic subdural hematoma," *Neurosurgical Review*, vol. 35, no. 2, pp. 155-169, 2012.
- [50] J. Gernsback, J. Kolcun and J. Jagid, "To drain or two drains: recurrences in chronic subdural hematomas," *World Neurosurgery*, vol. 95, pp. 447-450, 2016.

- [51] J. Fisher, J. Schwartzbaum, M. Wrensch and J. Wiemels, "Epidemiology of brain tumours," *Neurologic Clinics*, vol. 25, no. 4, pp. 867-890, 2007.
- [52] U. Kakarla, L. Kim, S. Chang, N. Theodore and R. Spetzler, "Safety and accuracy of bedside external ventricular drain placement," *Neurosurgery*, vol. 63, no. 1, pp. 162-166, 2008.
- [53] Y. Park, H. Woo, E. Kim and J. Park, "Accuracy and safety of bedside external ventricular drain placement at two different cranial sites: Kocher's point versus forehead," *Journal of Korean Neurosurgical Society*, vol. 50, no. 4, pp. 317-321, 2011.
- [54] C. R. Wirtz, F. K. Albert, M. Schwaderer, C. Heuer, A. Staubert, V. M. Tronnier, M. Knauth and S. Kunze, "The benefit of neuronavigation for neurosurgery analyzed by its impact on glioblastoma surgery," *Neurological Research*, vol. 22, no. 4, pp. 354-360, 2000.
- [55] W. J. Elias, J. B. Chaddock, T. D. Alden and E. R. Laws, "Frameless stereotaxy for transsphenoidal surgery," *Neurosurgery*, vol. 45, no. 2, pp. 271-275, 1999.
- [56] D. Orringer, D. Lau, S. Khatri, G. J. Zamora-Berridi, K. Zhang, C. Wu, N. Chaudhary and O. Sagher, "Extent of resection in patients with glioblastoma: limiting factors, perception of resectability, and effect on survival," *Journal of Neurosurgery*, vol. 117, no. 5, pp. 851-859, 2012.
- [57] A. Meola, F. Cutolo, M. Carbone, F. Cagnazzo, M. Ferrari and V. Ferrari, "Augmented reality in neurosurgery: a systematic review," *Neurosurgical Review*, vol. 40, no. 4, pp. 537-548, 2017.
- [58] I. Cabrilo, P. Bijlenga and K. Schaller, "Augmented reality in the surgery of cerebral aneurysms: a technical report," *Neurosurgery*, vol. 2, pp. 252-260, 2014.
- [59] W. Deng, F. Li, M. Wang and Z. Song, "Easy-to-use augmented reality neuronavigation using a wireless tablet PC," *Stereotactic and Functional Neurosurgery*, vol. 92, no. 1, pp. 17-24, 2014.
- [60] Chen, J. G, K. W. Han, D. F. Zhang, Z. X. Li, Y. M. Li and L. J. Hou, "Presurgical planning for supratentorial lesions with free Slicer software and Sina app.," *World Neurosurgery*, vol. 106, pp. 193-197, 2017.
- [61] G. C. Sun, F. Wang, X. L. Chen, X. G. Yu, X. D. Ma, D. B. Zhou, R. Y. Zhu and B. N. Xu, "Impact of virtual and augmented reality based on intraoperative magnetic resonance imaging and functional neuronavigation in glioma surgery involving eloquent areas," *World Neurosurgery*, vol. 96, pp. 375-382, 2016.

- [62] J. W. Yoon, R. E. Chen, K. ReFaey, R. J. Diaz, R. Reimer, R. J. Komotar, A. Quinones-Hinojosa, B. L. Brown and R. E. Wharen, "Technical feasibility and safety of image-guided parieto-occipital ventricular catheter placement with the assistance of a wearable head-up display," *International Journal of Medical Robotics and Computer Assisted Surgery*, vol. 13, no. 4, 2017.
- [63] M. Kersten-Oertel, I. Gerard, S. Drouin, K. Mok, D. Sirhan, D. S. Sinclair and D. L. Collins, "Augmented reality in neurovascular surgery: feasibility and first uses in the operating room," *International Journal of Computer Assisted Radiology and Surgery*, vol. 10, no. 11, pp. 1823-1836, 2015.
- [64] H. Brun, R. A. B. Bugge, L. K. R. Suther, S. Birkeland, R. Kumar, E. Pelanis and E. O. J, "Mixed reality holograms for heart surgery planning: first user experience in congenital heart disease," *European Heart Journal Cardiovascular Imaging*, 2018.
- [65] W. Si, X. Liao, Q. Wang and P. Heng, "Augmented reality-based personalized virtual perative anatomy for neurosurgical guidance and training," in *IEEE Conference on Virtual Reality and 3D User Interfaces*, Reutlingen, 2018.
- [66] T. Frantz, B. Jansen, J. Duernick and J. Vandemeulebroucke, "Augmenting Microsoft's HoloLens with vuforia tracking for neuronavigation," *Healthcare Technology Letters*, vol. 5, no. 5, pp. 221-225, 2018.
- [67] P. E. Pelargos, D. T. Nagasawa, C. Lagman, S. Tenn, J. V. Demos, S. J. Lee, T. T. Bui, N. E. Barnette, N. S. Bhatt, N. Ung, A. Bari, N. A. Martin and I. Yang, "Utilizing virtual and augmented reality for educational and clinical enhancements in neurosurgery," *Journal of Clinical Neuroscience*, vol. 35, pp. 1-4, 2017.
- [68] S. Issenberg, W. McGaghie, E. Petrusa, D. Lee Gordon and R. Scalese, "Features and uses of high-fidelity medical simulations that lead to effective learning: a BEME systematic review," *Medical Teacher*, vol. 27, no. 1, pp. 10-28, 2005.
- [69] F. Cutolo, A. Meola, M. Carbone, S. Sinceri, F. Cagnazzo, E. Denaro, N. Esposito, M. Ferrari and V. Ferrari, "A new head-mounted display-based augmented reality system in neurosurgical oncology: a study on phantom," *Computer Assisted Surgery*, vol. 22, no. 1, pp. 39-53, 2017.
- [70] J. R. Frank, L. S. Snell, O. T. Cate, E. S. Holmboe, C. Carraccio, S. R. Swing, P. Harris, N. J. Glasgow, C. Campbell, D. Dath, R. M. Harden, W. Iobst, D. M. Long, R. Mungroo, D. L.

- Richardson, J. Sherbino, I. Silver, S. Taber, M. Talbot and K. A. Harris, "Competency-based medical education: theory to practice," *Medical Teacher*, vol. 32, no. 8, pp. 638-645, 2010.
- [71] Royal College of Physicians and Surgeons of Canada, "Competence by design: reshaping Canadian medical education," 2014. [Online]. Available: <http://www.royalcollege.ca/rcsite/cbd/cbd-implementation-e>. [Accessed 17 April 2019].
- [72] E. S. Holmboe, J. Sherbino, D. M. Long, S. R. Swing, J. R. Frank and f. t. I. C. Collaborators, "The role of assessment in competency-based medical education," *Medical Teacher*, vol. 32, no. 8, pp. 676-682, 2010.
- [73] M. Kirkman, M. Ahmed, A. Albert, M. Wilson, D. Nandi and N. Sevdalis, "The use of simulation in neurosurgical education and training: A systematic review," *Journal of Neurosurgery*, vol. 121, no. 2, pp. 228-246, 2014.
- [74] C. Reiley, H. Lin, D. Yuh and G. Hager, "Review of methods for objective surgical skill evaluation," *Surgical Endoscopy*, vol. 25, no. 2, pp. 356-366, 2011.
- [75] P. Pratt, M. Ives, G. Lawton, J. Simmons, N. Radev, L. Spyropoulou and D. Amiras, "Through the HoloLens looking glass: augmented reality for extremity reconstruction surgery using 3D vascular models with perforating vessels," *European Radiology Experimental*, vol. 2, no. 1, p. 2, 2018.
- [76] N. Choudhury, N. Gelinias-Phaneuf, S. Delorme and R. Del Maestro, "Fundamentals of neurosurgery: virtual reality tasks for training and evaluation of technical skills," *World Neurosurgery*, vol. 80, no. 5, pp. e9-e19, 2013.
- [77] S. G. Hart and L. E. Staveland, "Development of NASA-TLX (Task Load Index): Results of Empirical and Theoretical Research," *Advances in Psychology*, vol. 52, pp. 139-183, 1988.
- [78] R. Vassallo, A. Rankin, E. Chen and T. Peters, "Hologram stability evaluation for Microsoft HoloLens," in *SPIE Medical Imaging*, Orlando, 2017.
- [79] M. Pfandler, M. Lazarovici, P. Stefan, P. Wucherer and M. Weigi, "Virtual reality-based simulators for spine surgery: a systematic review," *The Spine Journal*, vol. 17, no. 9, pp. 1352-1363, 2017.

Appendix A

Copy of Research Ethics Board Approval

The below document is a copy of the Queen's University Health Sciences & Affiliated Teaching Hospitals Research Ethics Board initial approval letter for the study entitled "Assessing the utility of holographic visualization for neurosurgery".



**QUEEN'S UNIVERSITY HEALTH SCIENCES & AFFILIATED TEACHING HOSPITALS
RESEARCH ETHICS BOARD (HSREB)**

HSREB Initial Ethics Clearance

January 11, 2018

Dr. Ron Levy
Department of Surgery
Kingston Health Sciences Centre
Room 226, Botterell Hall
18 Stuart Street
Kingston, Ontario K7L 3N6

ROMEO/TRAQ: #6022388

Department Code: SURG-413-17

Study Title: Assessing the utility of holographic visualization for neurosurgery.

**Co-Investigators: Dr. G. Fichtinger, Dr. A. Lasso, Dr. T. Ungi, Dr. Z. Keri, Ms. K. McIntosh,
Ms. E. Rae**

Review Type: Delegated

Date Ethics Clearance Issued: January 11, 2018

Ethics Clearance Expiry Date: January 11, 2019

Dear Dr. Levy,

The Queen's University Health Sciences & Affiliated Teaching Hospitals Research Ethics Board (HSREB) has reviewed the application and granted ethics clearance for the documents listed below. Ethics clearance is granted until the expiration date noted above.

- Protocol – Version: January 2, 2018
- Peer Review – Nov. 6, 2017
- Patient Information/Consent Form – Version 2
- Surgeon and Learner Information/Consent Form – Version 2

Documents Acknowledged:

- CORE Certificates – M. McIntosh and E. Rae

Amendments: No deviations from, or changes to the protocol should be initiated without prior written clearance of an appropriate amendment from the HSREB, except when necessary to eliminate immediate hazard(s) to study participants or when the change(s) involves only administrative or logistical aspects of the trial.

Renewals: Prior to the expiration of your ethics clearance you will be reminded to submit your renewal report through ROMEO. Any lapses in ethical clearance will be documented on the renewal form.

Completion/Termination: The HSREB must be notified of the completion or termination of this study through the completion of a renewal report in ROMEO.

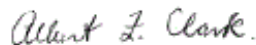
Reporting of Serious Adverse Events: Any unexpected serious adverse event occurring locally must be reported within 2 working days or earlier if required by the study sponsor. All other serious adverse events must be reported within 15 days after becoming aware of the information.

Reporting of Complaints: Any complaints made by participants or persons acting on behalf of participants must be reported to the Research Ethics Board within 7 days of becoming aware of the complaint.

Note: All documents supplied to participants must have the contact information for the Research Ethics Board.

Investigators please note that if your trial is registered by the sponsor, you must take responsibility to ensure that the registration information is accurate and complete.

Yours sincerely,



Chair, Health Sciences Research Ethics Board

The HSREB operates in compliance with, and is constituted in accordance with, the requirements of the Tri-Council Policy Statement: Ethical Conduct for Research Involving Humans (TCPS 2); the International Conference on Harmonisation Good Clinical Practice Consolidated Guideline (ICH GCP); Part C, Division 5 of the Food and Drug Regulations; Part 4 of the Natural Health Products Regulations; Part 3 of the Medical Devices Regulations, Canadian General Standards Board, and the provisions of the Ontario Personal Health Information Protection Act (PHIPA 2004) and its applicable regulations. The HSREB is qualified through the CTO REB Qualification Program and is registered with the U.S. Department of Health and Human Services (DHHS) Office for Human Research Protection (OHRP). Federabwide Assurance Number: FWA#:00004184, IRB#:00001173

HSREB members involved in the research project do not participate in the review, discussion or decision.

Appendix B

Copy of Research Ethics Board Amendment

The below document is a copy of the Queen's University Health Sciences & Affiliated Teaching Hospitals Research Ethics Board amendment letter for the study entitled "Assessing the utility of holographic visualization for neurosurgery".



**QUEEN'S UNIVERSITY HEALTH SCIENCES & AFFILIATED TEACHING HOSPITALS
RESEARCH ETHICS BOARD (HSREB)**

HSREB Amendment Acknowledgment/Ethics Clearance

March 22, 2018

Dr. Ron Levy
Department of Surgery
Kingston Health Sciences Centre
Room 226, Botterell Hall

ROMEO/TRAQ: #6022388
Department Code: SURG-413-17
Study Title: Assessing the utility of holographic visualization for neurosurgery.
Review Type: Delegated
Date Ethics Clearance Issued: March 22, 2018

Dear Dr. Levy,

The Queen's University Health Sciences & Affiliated Teaching Hospitals Research Ethics Board (HSREB) has reviewed the amendment application and granted ethics approval/acknowledgement for the documents listed below.

- Addition of Zachary Baum and Sarah Ryan to the study team
- CORE Certificates – Z. Baum and S. Ryan
- Protocol – Version: March 21, 2018
- Patient Research Participant Information/Consent Form – Version: March 21, 2018
- Surgeon and Learner Research Participant Information/Consent Form – Version: March 21, 2018
- Protocol – Version: March 21, 2018

Yours sincerely,

Albert J. Clark

Chair, Health Sciences Research Ethics Board

The HSREB operates in compliance with, and is constituted in accordance with, the requirements of the Tri-Council Policy Statement: Ethical Conduct for Research Involving Humans (TCPS 2); the International Conference on Harmonisation Good Clinical Practice Consolidated Guideline (ICH GCP); Part C, Division 5 of the Food and Drug Regulations; Part 4 of the Natural Health Products Regulations; Part 3 of the Medical Devices Regulations, Canadian General Standards Board, and the provisions of the Ontario Personal Health Information Protection Act (PHIPA 2004) and its applicable regulations. The HSREB is qualified through the CTO REB Qualification Program and is registered with the U.S. Department of Health and Human Services (DHHS) Office for Human Research Protection (OHRP). Federalwide Assurance Number: FWA#:00004184, IRB#:00001173

HSREB members involved in the research project do not participate in the review, discussion or decision.